IS-3634

CONF—720515--5

HYDROGEN EMBRITTLEMENT AND OTHER EFFECTS IN THERMONUCLEAR REACTOR MATERIALS

T. E. Scott

AMES LABORATORY, USERDA
IOWA STATE UNIVERSITY
AMES, IOWA

Date Transmitted: June 1975

PREPARED FOR THE U. S. ENERGY RESEARCH AND DEVELOPMENT ADMINISTRATION
UNDER CONTRACT W-7405-eng-82

DISCLAIMER

IS-3634

HYDROGEN EMBRITTLEMENT AND OTHER EFFECTS IN THERMONUCLEAR REACTOR MATERIALS

T. E. Scott

Ames Laboratory, ERDA
Iowa State University
Ames, Iowa 50010

Date Transmitted: June 1975

PREPARED FOR THE U.S. ENERGY RESEARCH AND DEVELOPMENT ADMINISTRATION UNDER CONTRACT NO. W-7405-eng-82

Invited paper presented in a special technical session on Controlled Thermonuclear Materials at the Spring Meeting of The Metallurgical Society of AIME, Boston, Mass., 1972.

Available from: National Technical Information Service
U. S. Department of Commerce
P.O. Box 1553
Springfield, VA 22161

Price: Microfiche $2.25

Distribution List

T. E. Scott	10
Ames Lab - Library	10
ERDA-TIC	27

ABSTRACT

Current fusion reactor design concepts are based on deuterium-tritium plasma fuel. The fuel and possible internal proton creation by (n,p) reactions provide sources of hydrogen isotopes which may have serious deleterious effects on the integrity of containment materials in a thermonuclear reactor. This paper considers the potential deleterious effects of hydrogen isotopes on the mechanical behavior of candidate containment materials, such as vanadium, niobium, molybdenum and others. Current knowledge of hydrogen-induced embrittlement in these metals is reviewed in relation to CTR application and other potential material problems caused by hydrogen isotopes under fusion reactor operating conditions are indicated. Related information such as hydrogen solubility, hydrogen-metal phase diagrams, and hydrogen diffusivity are included.

THIS PAGE

WAS INTENTIONALLY

LEFT BLANK

I. Introduction

Current designs of projected controlled thermonuclear reactors, hereafter denoted CTR, are based on the deuterium-tritium (D-T) fuel cycle for several reasons: The D-T mixture has the lowest ignition temperature known;[1] it has the highest reaction rate;[2] it offers a pessimistic situation because it involves tritium as an environmental hazard;[2] and many of the problems associated with it appear similar to problems in alternate fuel cycles[3].

Since tritium is rare - it would take the entire world's supply[2] of 10 kg just to get a CTR started at an estimated[4] cost of 1 million dollars per kg - it is necessary to produce tritium, by breeding, in excess of the amount consumed in the D-T fusion reaction so that CTR's can be considered an economically viable source of power. Thus a finite tritium inventory must exist in a CTR system. The tritium inventory in the breeding blanket, the D-T fuel, and the protons created in the structural material by (n,p) reactions present a potentially serious materials integrity problem that will have to be dealt with in CTR design and ultimate operation.

Even without an established design for the projected CTR, it is evident that the effect of hydrogen and its isotopes on the mechanical behavior of the first wall material and other structural components is a potential design limiting factor.

A diagram of a conceptual CTR core structure, taken largely from the design of Fraas and Postma[5], is shown in Fig. 1. Cylindrical walls with struts in the coolant zone have been

indicated, although the design of Fraas employs a modular structure to avoid buckling instabilities. The simpler form was used here for clarity. It is believed that Fig. 1 illustrates the essential features of the design that are pertinent to hydrogen problems; it is not meant to suggest that this would be the ultimate design for CTR's.

Little information concerning the effects of tritium or deuterium on the mechanical behavior of materials exists. Accordingly, it is necessary to assume that the effects of hydrogen will provide a reasonably accurate picture of what problems to expect from its isotopes. Hence, in the following the use of the term hydrogen will be meant to include tritium and deuterium.

Neutronic properties and mechanical strength requirements for the CTR operating temperature range, 600°C to 1000°C, tend to favor vanadium, niobium, molybdenum or their alloys for the first wall material. Since CTR prototypes are likely to be built and used for experimentation at lower temperatures before full-scale operations are constructed, it is worthwhile to consider austenitic stainless steels and perhaps titanium, zirconium and yttrium alloys in the context of this paper. Accordingly, the remainder of the text will consider the potential effects of hydrogen on the mechanical behavior of the metals and alloys just named.

The sources of hydrogen will be discussed, then a summary of the current state of our knowledge regarding low temperature (<300°C) hydrogen embrittlement of the metals and alloys previously mentioned will be presented because this will be important

during CTR shut-down procedures. Several hydrogen effects that could occur at CTR operating temperatures will be indicated and their probability of occurrence and potential seriousness with respect to CTR operation will be evaluated.

II. Sources of Hydrogen Isotopes in the First Wall

This paper is concerned primarily with the first wall region including the vacuum, coolant and structure. An enlarged view of this region is shown schematically in Fig. 2 which attempts to give some idea of the conditions that are likely to prevail.

Virtually all the potential first wall material degrading phenomena depend on the concentration of hydrogen isotopes in the wall. This concentration will depend on the hydrogen isotope concentration in the blanket, the gas pressure on the vacuum side, the neutral isotope flux from the plasma to the wall and on the protons generated by neutron captures of the (n,p) type in the wall. Other neutron capture reactions can produce hydrogen isotopes but the quantity expected is minor compared to the protons. Where this is not true, the additional reactions have been lumped with the (n,p) reactions to estimate total hydrogen isotope generation. In the following, an attempt is made to estimate hydrogen isotope concentrations in the wall from each of the sources just mentioned.

II-1. From the Blanket

As was mentioned above, the CTR's must maintain a finite tritium inventory in the blanket in order to be economically feasible. The source of tritium for the inventory is through

breeding by way of $^{6}Li(n,\alpha)T$ and $^{7}Li(n,\alpha n')T$ reactions. The inventory will depend on the tritium extraction efficiency which involves the rate of coolant cycling. (Note: The tritium extraction cycle, another region of potential hydrogen isotope problems, will not be discussed here).

The partitioning of tritium between the blanket and the wall will depend on the equilibrium tritium partial pressure over the lithium coolant at appropriate temperatures. This pressure will depend on the amount of tritium in the lithium blanket. Analyses[4-6] suggest a tritium inventory of the order 0.05 atom percent (a/o) or 0.002 a/o is desirable. Adequate equilibrium P-T-C data for the lithium-hydrogen exist[7,8] at the temperatures of CTR operation. But, data do not exist for the compositions that are expected[4-6]. Furthermore, lithium-hydrogen P-T-C equilibrium data are not available for temperatures below about 700°C and this information could be important as will be indicated later. Fig. 3 is a schematic Li-LiH phase diagram from Messer[7]. The cross-hatched region on the left-hand side of the diagram depicts an exaggerated version of the expected CTR temperature and tritium concentration range. Some equilibrium partial pressure-composition data for the Li-T and Li-H system are available for a few temperatures in the CTR range[7,8] as shown in Fig. 4. Since these data do not extend to the low concentration range expected in the CTR blanket, it is necessary to extrapolate the existing data. Consequently, the 700°C data of Fig. 4 from Heumann and Salmon[8] were replotted in the form of log pressure versus log hydrogen concentration as shown in Fig. 5. It is evident that excessive

extrapolation is required to reach the expected CTR concentration range indicated near the lower left-hand corner of the figure. It is also clear that Sievert's law is not obeyed by the experimental data. Failure of Sievert's law makes it impossible to extrapolate the data in a meaningful way. In order to estimate the equilibrium pressure at the low CTR concentrations, the author assumed that Sievert's law would hold at concentrations lower than the existing data. Lines intersecting the existing data plots and their extrapolation were drawn in to conform with Sievert's law (slope = 2). The latter are shown as lighter lines in Fig. 5. The most favorable situation, i.e., low equilibrium pressure, is obtained by assuming that Sievert's law begins to be obeyed at the lowest existing data point while the least desirable case is given by the linear log-log extrapolation of the existing data for tritium. The most likely situation would probably be obtained by assuming Sievert's law becomes valid at about 1 a/o hydrogen or tritium. Fig. 5 also shows a list of the equilibrium pressures for the most favorable, likely and least favorable situations for the two tritium concentrations suggested by Fraas[4,5]. The range is from roughly 10^{-6} torr to 0.25 torr but the most likely equilibrium partial pressure range is probably between 10^{-6} and 10^{-3} torr. It would seem a bit premature to attempt a more exact figure at this time or until lower concentration data are obtained.

II-2. From the "Vacuum" Side of the Wall

There are two, perhaps related, sources of hydrogen isotopes from the vacuum side of the first wall. These are the current of

neutral deuterium and tritium particles from the plasma and the gas in the region adjacent to the wall. According to Steiner's[9] summary of the present knowledge, a gas pressure of 10^{-6} to 10^{-2} torr might be expected. To be conservative this gas should probably be assumed to consist entirely of hydrogen isotopes.

The current of neutral deuterium and tritium particles incident on the wall is anticipated to be 10^{14} to 10^{16} particles/cm^2-sec., depending on the plasma confinement time, at an energy of about 20 keV if the effect of gas adjacent to the wall is neglected[9]. A justifiably crude approximation, assuming the maximum depth of penetration or range of the energetic isotopes is 1000Å,[10] indicates that these currents would deposit an average concentration of 10^{-2} to 3 atom percent of deuterium and tritium per second in the 1000Å skin nearest the plasma (Table I). It should be cautioned that the above estimate assumed that the total current of particles is trapped. However, McCracken[11] found that the trapping efficiency varied with the heat of solution and temperature. Backscattering reduces the total effective flux. Naturally the deuterium and tritium will tend to escape the wall by diffusion and a steady-state concentration will be reached. The steady-state concentration and distribution will depend on the equilibrium solubility of the isotopes in the material which in turn depends

on the pressure on either side of the wall. Neglecting all other sources of isotopes, a concentration, peaking at about the depth of maximum penetration, can be estimated by equating the particle current, I_p, to the diffusion flux, J, which is given by Fick's first law if the concentration, C, is in units of atoms/cc. Thus,

$$I_p = J = D \frac{dC}{dX} .$$

Letting $\frac{dC}{dX} \simeq \frac{C_{max}}{X_{max}}$, where X_{max} is the maximum penetration depth and C_{max} is the concentration at the peak in units of atoms/cc, and setting $D \simeq 10^{-4}$ cm^2/sec, $I_p \simeq 10^{15}$ isotopes/cm^2-sec and $X_{max} \simeq 10^{-5}$ cm, the value of C_{max} is about 10^{14} isotopes per cm^3 of metal ($\approx 10^{-7}$ atom percent). Thus, unless the isotopes are prevented from escaping, the expected steady-state peak concentration should be acceptably low from this source even though the estimate is probably no better than $\pm$ 2 orders of magnitude.

II-3. From Neutron Capture Reactions in the Wall

The major source of hydrogen from neutron captures in the first wall is the (n,p) reactions. If the neutron flux of 3.7×10^{15} cm^{-2} - sec^{-1} through the wall is accepted and it is assumed that about one-fourth of this flux is at 14 MeV[12], an approximate proton generation rate can be calculated. Using the (n,p) cross-sections[13] given in Table II, the hydrogen concentrations generated per second have been determined for the materials of interest (Table II). If the hydrogen production rates indicated were continued for a month with no concomitant loss, the resulting concentration would constitute a serious materials

problem in the form of blisters, internal fissuring and embrittlement during cool-down at least.

However, the low solubilities (Figs. 6-12) and high diffusivities (Figs. 13 and 14) of hydrogen in these materials would probably not permit such concentrations to develop. A reasonably accurate estimate of the hydrogen concentrations attainable from this source can be made by assuming steady-state conditions for an infinite slab (approximating the first wall) with concentration C_o on the blanket side and concentration C_1 on the plasma side with a volumetrically uniform constant proton source from (n,p) reactions, $\dot{R}$. This problem is similar to heat flow from an infinite slab with uniform internal heating. The generalized equation resulting from a mass balance at steady state is:

$$-D\nabla^2 C = \dot{R}(\bar{r})$$

For the planar approximation of interest here this reduces to:

$$-D\left(\frac{d^2C}{dX^2}\right) = \dot{R} = \left[\frac{\dot{H}}{M}\right]$$

The solution, when $\dot{R}$ is constant independent of position for the boundary conditions prevailing, is:

$$C(X) = \frac{-\dot{R}X^2}{2D} + \left(\frac{C_1-C_o}{L} + \frac{\dot{R}L}{2D}\right) + C_o$$

where D = diffusivity, $\dot{R}$, C_1 and C_o as defined above and L is the wall thickness. Maximizing this expression leads to:

$$X_C(C_{max}) = \frac{D}{\dot{R}L}(C_1 - C_o) + \frac{L}{2}$$

$$\text{and } C_{max} = \frac{D}{2\dot{R}L^2}(C_1 - C_o)^2 + \frac{C_1 + C_o}{2} + \frac{\dot{R}L^2}{8D}$$

Since the values of C_1 and C_o will depend on the equilibrium partial pressures of hydrogen on either side of the wall and these are unspecified, an estimate of the concentration is best obtained by assuming $C_1 = C_o = 0$. Then:

$$C_{max} = \frac{\dot{R}L^2}{8D} = \left[\frac{H}{M}\right]_{max}$$

Taking L = 0.5 cm, picking the diffusivities at about 700°C from Figs. 13 and 14 and the values of $\dot{R}$ given in Table II the values of C_{max} listed in the fourth column of Table II are obtained. All the values are of the order of 1 ppm atomic or less. Examination of the solubilities in Figs. 6-12 reveals that the contribution of hydrogen from (n,p) reactions is either much less than the concentrations C_1 and C_o or that the combined (n,p) generated hydrogen and the equilibrium solubility is ~1-10 ppm atomic (e.g. molybdenum). Accordingly, it seems that (n,p) reactions in the wall will not contribute hydrogen concentrations significantly above those in equilibrium with the hydrogen pressure (10^{-6} to 10^{-3} torr) on either side of the wall.

At this point a summary of the hydrogen isotope sources and the quantities of isotopes they generate is in order. Unfortunately, all quantities are only best estimates based on anticipated conditions. Tritium concentrations of the order

0.002 to 0.05 atom percent in liquid lithium coolant will have estimated equilibrium partial pressures between 10^{-6} to 10^{-3} torr. On the plasma side of the first wall pressures of 10^{-6} to 10^{-2} torr may exist. For safety sake this gas pressure is assumed to be tritium and deuterium. From the plasma, escaping neutral atoms of deuterium and tritium will bombard the wall at a current of 10^{14} to 10^{16} atoms/cm^2-sec. These atoms injected into the wall to a depth of about 1000Å will produce an estimated concentration of hydrogen isotopes of about 10^{-7} atom percent assuming diffusion controlled escape from the wall. However, surface effects may control, and the hydrogen isotope build-up under these conditions are, at present, difficult to determine because the surface controlling mechanism is not known. At the extreme condition of complete surface blocking on the plasma side but diffusion controlled desorption on the blanket side, a steady-state average concentration of about 50 atom percent would develop. Finally, the production of protons in the wall from (n,p) reactions will amount to concentrations of the order 1 ppm atomic at steady state. Again, however, surface blocking could permit damaging quantities of hydrogen to build up.

III. Low Temperature (<300°C) Hydrogen Embrittlement

III-1. Niobium and Vanadium

Niobium and vanadium (also tantalum) are catastrophically embrittled by relatively low concentrations of dissolved hydrogen near room temperature. This fact is well documented[30-47]. Researchers differ about such things as whether ductility is

returned at liquid nitrogen temperature and whether hydride or hydrogen in solution causes the embrittlement. However, there is no argument about the increased ductile-brittle transition temperature (DBTT) induced by the presence of hydrogen. This is the important concern for CTR design and safe operation.

No attempt will be made to critically review or discuss the mechanisms suggested for hydrogen embrittlement of the metals. Rather, only the characteristics of the DBTT as affected by hydrogen concentration will be indicated and discussed in terms of CTR operation. Fig. 15 illustrates the general features of the ductility as it varies with test temperature for either niobium or vanadium containing dissolved hydrogen. It is evident that, for a fixed hydrogen content the reduction in area (R.A.) drops off gradually as the test temperature is decreased to some critical value, at which point it drops more sharply, depending on the hydrogen content, to virtually zero ductility. Depending on the hydrogen content, the ductility may return to substantial values (~60% R.A.) at the temperature of liquid nitrogen. At higher hydrogen contents the ductility does not return at low temperatures. This phenomenon and its explanation are not important for the considerations at hand.

The general characteristics of R.A. vs temperature curves for increasing hydrogen contents are shown in Fig. 16 for vanadium. Tantalum and niobium behave similarly. It is clear that the nature of the DBTT region changes as the hydrogen content increases. The ductile-brittle transition appears to become less sharp as the

hydrogen content is increased. The dependence of DBTT on hydrogen content is illustrated graphically in Fig. 17. Because the initial gradual drop in R.A. makes it difficult to decide what temperature to assign to the transition, it has been arbitrarily selected as that temperature where the R.A. has dropped to half the value of the hydrogen-free vanadium. Included in Fig. 17 are the results of Longson[42] for niobium.

It should be mentioned that hydrides do form in these metals and that there appears to be a subtle relation between the hydride formation temperature and the DBTT. However, the available phase diagrams (Figs. 18 and 19) for vanadium-hydrogen and niobium-hydrogen indicate a critical temperature above which no hydride forms. The question then arises: Does the low temperature embrittlement and its associated DBTT behavior persist above the critical temperature where all the hydrogen is in solution? The answer would appear to be yes for niobium, based on the results of Walter and Chandler[44] and of Longson[42]. They both show DBTT behavior above the critical temperatures shown. Data for vanadium have not been determined at sufficiently high temperatures but, if we accept the similarity between niobium and vanadium and note the results of Longson in Fig. 17, it seems that vanadium would also exhibit the DBTT behavior above the critical temperature providing the hydrogen concentration was high enough.

III-2. Molybdenum and Austenitic Stainless Steel

The available experimental evidence indicates that molybdenum[50] is not embrittled by hydrogen at low temperatures although there has been reported a reduction of ductility at room temperature for

specimens exposed to hydrogen at elevated temperatures (800°C)[51]. However, it appears that this reduction of ductility is a result of degradation at the elevated temperature rather than hydrogen embrittlement at room temperature.

With regard to austenitic stainless steel there are some conflicting interpretations[52-68], but it seems that stable austenitic stainless steels are not significantly embrittled at low temperatures by hydrogen.

III-3. Titanium, Zirconium and Yttrium

The effects of hydrogen at low temperature on alpha, alpha-beta and beta titanium[69-79] and alpha and alpha-beta zirconium[80-87] have received considerable attention. The behavior of these metals and their alloys are quite similar. Two types of embrittlement caused by hydrogen in these metals have been established: one, impact embrittlement is associated with hydride plates and is accentuated by low temperatures and high strain rates; the other is characterized as a low strain rate embrittlement similar to hydrogen embrittlement of steels and has been attributed by some as being caused by dissolved hydrogen. Regardless of the mechanism both metals exhibit low temperature hydrogen-induced embrittlement.

To the author's knowledge no complete or systematic study of the effects of hydrogen on the ductility of yttrium has been conducted. Nevertheless, the characteristics of yttrium being similar to titanium and zirconium, analogous effects of hydrogen are expected.

III-4. Evaluation of the Probability of Low Temperature Hydrogen Embrittlement under CTR Conditions

This particular phenomenon will be a problem only during the

CTR shut-down operations assuming that temperatures will be dropped to near room temperature. In order to assess the probability of embrittlement, we must compare the hydrogen concentration required for the DBTT to be raised above room temperature (Fig. 17) with the concentration in equilibrium with hydrogen gas pressures in the 10^{-6} to 10^{-3} torr range (Figs. 6 and 7) for vanadium and niobium. Fig. 17 shows that the DBTT is room temperature at hydrogen concentrations near 1.4 atom percent (~150 ppmw) for niobium and at 2.7 atom percent (~550 ppmw) for vanadium. According to Figs. 6 and 7 these concentrations are easily reached at room temperature for hydrogen gas pressures of 10^{-6} to 10^{-3} torr. It was already mentioned that molybdenum and stable austenitic stainless steels are immune to this type of embrittlement. On the other hand, titanium, zirconium and yttrium will contain hydrides at room temperature in the hydrogen gas pressure range of concern as shown in Figs. 10-12. Therefore, their ductilities can be expected to be reduced.

The hydrogen gas pressure range being considered is that over Li-H at 700°C. The equilibrium pressure range at 1000°C will be higher, but at lower temperatures, especially approaching room temperature, the equilibrium hydrogen pressure will be considerably lower. Until data for the Li-H system and the wall material - hydrogen systems in the appropriate ranges are available it would not be wise, from the safety point of view, to consider that low temperature hydrogen embrittlement of some of the potential wall materials is of little concern. At the current state of knowledge, it would be advisable to extract the hydrogen

isotopes (tritium) from the lithium and plasma zone before cooling down.

IV. Hydrogen Isotope Effects in the CTR Operating Range

The effects of hydrogen at low pressures (<1 torr) on metals in the CTR operating range (600°C to 1000°C) are virtually unexplored. Consequently, the hydrogen-induced first wall material degrading effects itemized below are only potential problems envisioned by the author.

IV-1. Hydrogen Embrittlement at CTR Temperatures

By this is meant a continuance into the higher temperature range of the type of embrittlement observed at low temperature. Since the mechanism of low temperature hydrogen embrittlement is not established, it is impossible to say that it will not occur at higher temperatures than have been investigated to date. However, several factors can be mentioned which should help to evaluate the probability of this type of material degradation. Whether it is hydrogen in solution or as precipitated hydride or in some undetermined distribution that produces the catastrophic embrittlement, the fact remains that the enhanced ductility of the matrix at higher temperatures will mitigate the tendency for cleavage crack propagation. Furthermore, extrapolation from the low temperature range (Fig. 17) indicates that substantial hydrogen concentrations would be necessary to produce a ductile to brittle transition in niobium or vanadium and that the concentration of hydrogen required for hydride formation in titanium, zirconium and yttrium would be high. Also, the hydride of

titanium becomes ductile[79] above about 300°C thereby reducing the embrittling tendency of the hydrides. For example, Fig. 17 shows that about 36 atom percent (6000 ppmw) hydrogen in niobium and about 93 atom percent (2×10^5 ppmw) in vanadium would be required to raise the DBTT to the CTR temperature range. According to Fig. 6 and 7 these concentrations of hydrogen could not be attained from the hydrogen gas pressures suggested in section II, viz., 10^{-6} to 10^{-3} torr. However, conditions in the surface of the wall near the plasma could attain compositions high enough due to energetic isotope injection if outgassing could not occur. This is discussed more thoroughly in section IV-2 where it is shown that blistering would probably occur rather than brittleness.

In regard to titanium, zirconium and yttrium, which appear to be embrittled by hydrides, it should be noted that the hydrides will tend to dissociate over most of the CTR temperature range. So, unless solution hydrogen can embrittle these metals, embrittlement would not be anticipated.

If the low temperature behavior of stable austenitic stainless steel and molybdenum prevails, these metals also should not be embrittled by hydrogen at CTR temperatures.

IV-2. Blistering

Blistering is the localized bulging of the surface of a metal caused by internal gas pressure as illustrated schematically in Fig. 20. This process would not normally occur under equilibrium conditions. However, when a metal is super-charged with gas atoms,

the atoms can combine, usually at lattice discontinuities such as grain boundaries, radiation induced voids, helium bubbles, second phase particle interfaces, etc., to form the molecular gas phase at a pressure in local equilibrium with the supersaturated matrix. This local equilibrium pressure frequently is extremely high, causing the metal to deform. At the surface this produces blisters while, internally, fissures can be formed.

The CTR first wall is subjected to two sources of non-equilibrium hydrogen isotopes: The injected energetic tritium and deuterium and the protons created internally by (n,p) reactions. Even with high mobilities it is possible for these non-equilibrium isotope atoms to be trapped at lattice discontinuities of the type cited above. Thus the atoms could combine and produce blistering. These blisters could effect heat transport, leading to hot spots, or they could eventually rupture, reducing the local wall thickness, and emit their contents to the plasma zone.

The blistering phenomenon is well documented[88-91] for steels charged with hydrogen at high temperatures, then quenched to room temperature where the equilibrium solubility is much less and for steels charged with hydrogen electrolytically at ambient temperature because very high effective pressures are developed at the steel specimen cathode.

Based on the analysis in section II-2 of the maximum concentration, C_{max}, developed by injection of neutral deuterium and tritium and the expected proton levels from (n,p) reactions con-

sidered in section II-3, it would not seem likely that blisters would form under CTR conditions in the first wall candidate materials. For example, if it is assumed that an internal pressure of 5000 psi (2.6×10^5 torr) would be required to cause blistering, the local super-concentration of isotope atoms would have to be substantial as shown by Figs. 6-12. The results of the analyses in section II indicate that these concentrations would never be attained. However, recent experiments have revealed blisters numbering 6×10^6 cm^{-2} in niobium which had been bombarded with deuterium at CTR temperatures[92,93]. In view of the contradiction between experiment and analysis, it must be admitted that diffusing isotope atoms encounter very efficient traps near the surface with significant frequency to produce blistering of serious proportions. Apparently, it is not simple volume diffusion that controls the emission or out-gassing kinetics.

While no test of the blistering propensity of the hexagonal metals titanium, zirconium or yttrium has been performed, it would seem that the phenomenon would be minimal in these metals. All of them form hydrides which are stable to temperatures approaching CTR range. Even at the high side of anticipated CTR temperatures where the hydrides of these metals will dissociate, the pressures will not be high.

The tendency to blister should increase with decreasing solubility of the hydrogen isotopes and with decreasing diffusivity. However, as noted above, surface effects may dominate and these

are very difficult to anticipate. In summary, blistering due to hydrogen isotopes introduced by particle bombardment and (n,p) reactions should be acknowledged as a potentially serious first wall degrading phenomenon. Systematic investigations of this problem should be given consideration.

IV-3. Internal Hydriding

The problem of internal hydriding would not exist for wall materials made of pure metals. However, the creep and tensile properties required for the CTR operating temperature range demand that the materials being considered, with the possible exception of molybdenum, must be strengthened by alloying. Typical of the alloys currently known are Nb-5V-1.25Zr, Nb-10Ti-5Zr, Nb-1Zr, V-1 to 20Ti, V-Ti and Mo-0.5Ti-0.1Zr.

The requirements for a system to exhibit internal hydriding are: (a) the solute must have a higher affinity for hydrogen than the matrix, (b) the matrix must have a finite hydrogen solubility, and (3) the diffusivity of hydrogen must be higher in the matrix than that of the metallic solute species. These conditions appear to be satisfied for the alloy systems just mentioned. A schematic illustration is provided by Fig. 21.

It is possible that internal hydriding could improve the high temperature creep and tensile properties. On the other hand, if the necessary high temperature mechanical properties are derived from second phase particles whose stability is low with respect to the hydrides, then the latter will form at the expense of the hardening phase. Depending on the relative strengthening effects

of the hydride phase and the intentional second phase, the system could be strengthened or weakened. In addition to the mechanical property effects just mentioned, there is another effect of internal hydriding which seems to be only detrimental. It has been shown[94] that alloy additions, e.g., titanium to vanadium, can mitigate radiation induced void formation. Internal hydriding of the alloy addition would reduce its effectiveness in this process. On the other hand, zirconium as a transmutation product of niobium might be hydrided with the result that properties could be improved.

Finally, if internal hydriding occurs in the CTR operating temperature range without deleteriously affecting the properties, the effect of the hydride second phase on the ductility of the wall material during reactor cool-down must be considered. For example, molybdenum containing titanium hydride particles might have impaired ductility near room temperature due to thermal stresses around the hydride particles.

To evaluate the probability of internal hydriding in candidate first wall materials the thermodynamics of the following type of chemical reaction must be examined.

$$(I) \qquad M(T,P) + [S]_M(N_S,T,P) + X[I]_M(N_I,T,P) \rightarrow M(T,P) + SI_X(T,P)$$

where M = matrix element or solvent element, e.g., Molybdenum

$[S]_M$ = substitutional solute dissolved in solvent, e.g., zirconium in molybdenum.

$[I]_M$ = interstitially dissolved gas atom, H isotopes in this case.

T,P = usual significance

N_S = atom fraction of substitutional solute

N_I = atom fraction of dissolved gas atoms

The free energy change for this reaction, assuming the total pressure, P, is one atmosphere is:

$$\Delta G_R = \mu_{SI_x}(T) - \mu_{[S]_M}(N_s,T) - X\mu_{[I]_M}(N_I,T)$$

or in different form:

$$\Delta G_R - \Delta G^\circ = RT \ln \left[\frac{a_{SI_x}}{a_{[S]} \cdot a^x_{[I]}}\right]$$

For facility in obtaining tabular data we chose as the standard reaction the following:

$$S(\text{solid}, T) + \frac{X}{2} I_2(g,T) \rightarrow SI_x\ (\text{Solid}, T)$$

Since the standard reaction data are usually tabulated for $T = 298°K$ a free energy term must be added to the standard reaction free energy at 298°K to raise it to T. Since this is primarily an entropy change we can assume the change for the solid phases, S and SI_x, are negligible and deal only with the change for the gas phase. Therefore,

$$\Delta G^\circ_T = \Delta G^\circ_{298} + \Delta G$$

where $\Delta G = \frac{X}{2}\left[\mu_{I_2}(g,T) - \mu_{I_2}(g,298)\right]$

and this can be obtained from thermodynamic tables.

To be consistent with the temperature taken for the Li-H system, the internal hydriding situation is examined for 700°C (973°K). At equilibrium, $\Delta G_R = 0$. Therefore

$$\Delta G_T^\circ = -RT \ln \left[\frac{a_{SI_x}}{a_{[S]} \cdot a_{[I]}^x} \right].$$

Since the composition of SI_x is virtually constant let $a_{SI_x} = 1$ and assume the metal-solute system is ideal so that $a_{[S]} = N_S$ and that Sievert's law holds for the gas species so that $a_{[I]}^x = P_{I_2}^{x/2}$. Therefore:

$$\Delta G_T^\circ = RT \ln \left[N_S \cdot P_{I_2}^{x/2} \right]$$

or $$P_{I_2} = \left[\frac{1}{N_S} e^{\frac{\Delta G_T^\circ}{RT}} \right]^{2/X}$$

Typical of the alloys which might be used for the first wall material are:

Mo + 0.1 Zr

Mo + 0.5 Ti

Nb + 1 Zr

V + 20 Ti

The hydrides of zirconium and titanium are ZrH_2 and TiH_2; thus, X = 2 in the above equation and S = Zr or Ti and I = H. Therefore:

$$\Delta G = \mu_{H_2}(g,T) - \mu_{H_2}(g,298)$$

Appropriate data from Fast[95] for T = 1000°K (close enough to 973°K) for H_2(gas) are:

$h_T^\circ - h_{298}^\circ = 4940$ cals/mole, $(S_T^\circ - S_{298}^\circ) = 8.49$ cals/deg-mole

and $S_{298}^\circ = 31.21$ cal/deg-mole. This gives

$$\Delta G = \mu_{H_2}(T) - \mu_{H_2}(298) = (h_T^\circ - h_{298}^\circ) - T(S_T^\circ - S_{298}^\circ) - (T-298)S_{298}^\circ$$

$= +25{,}460$ cals/mole

Therefore for all dihydride systems:

$$\Delta G_T^\circ = \Delta G_{298}^\circ + 25{,}460 \text{ cals/mole}$$

From Libowitz[96]: $\Delta G_{298}^\circ\ (ZrH_2) = -29{,}300$ cals/mole

and $\Delta G_{298}^\circ\ (TiH_2) = -20{,}000$ cals/mole. Using these values, the standard reaction free energies, ΔG_T°, at 700°C (973°K) are:

$$\Delta G_T^\circ\ (TiH_2) = +5460 \text{ cals/mole}$$

$$\Delta G_T^\circ\ (ZrH_2) = -3840 \text{ cals/mole}$$

Thus, for ZrH_2 at 700°C,

$$P_{H_2}\ (\text{torr}) = \frac{760}{N_s} \exp\left[\frac{-3840}{1946}\right] = \frac{106}{N_s}$$

Since N_s can't be greater than unity, it is clear that the hydrogen pressures required for internal hydriding of zirconium are much larger than those expected in the CTR. Furthermore, TiH_2 is unstable at 700°C and ZrH_2 is just barely stable and would become unstable at a slightly higher temperature. For example, at 600°C, the dissociation pressures of ZrH_2 and TiH_2 are 0.93 torr and 52 torr respectively[97]. Consequently, the likelihood of internal hydriding under CTR conditions seems remote for the first wall material. If temperatures at the second wall are substantially lower than at the first wall internal hydriding may be an important factor there.

IV-4. Hydrogen Reaction with Other Impurities

The type of degradation implied here involves chemical reaction of hydrogen with other impurities to form gaseous reaction products. Rogers[98] has called this hydrogen attack. Classic examples are found in copper[99-103] silver[104-106] and steels[107-111]. In copper and silver hydrogen diffuses into the metal and combines chemically with the oxygen of the respective oxides to produce water vapor which, above the critical temperature for water of ≈375°C, produces high gas pressures. The pressure and linking-up of bubbles produces inter- and intragranular fissuring. Or, if this occurs near the surface, the fissures are expanded by the gas pressure to produce blisters or surface upheavals similar to those discussed earlier. In steels, it has been found that methane[111] forms by combination of hydrogen with carbon. This has the combined effect of depleting the carbides and producing fissures. Grain boundary fissuring due to the interaction of hydrogen and oxygen in iron has also been observed[110].

The fact that such processes occur in the above-mentioned metals does not mean a priori that they will occur in the metals likely to be used for the first wall in a CTR. However, it serves as a warning that such degrading effects are possible. For example, there is evidence[51] that molybdenum, exposed to hydrogen for 4 hours at 10^{-5} torr pressure at 800°C followed with 6 hours in vacuo at 5×10^{-7} torr at the same temperature,

had reduced properties when tested at 25°C. Furthermore, results have been reported[44] which indicated that argon atmospheres containing as little as 2% H_2 can decarburize molybdenum.

Of course, whether such processes will occur depends on the relative thermodynamic stability of other impurity phases with respect to hydrogen. This, in turn, will depend, among other things, on temperature and hydrogen pressure. Generally hydrogen attack has been observed in rather high hydrogen pressures ($\geq$1 atmosphere).

The type of reaction considered here is, for example,

$$(II) \quad [N]_N^{Sat} + 3[H]_{Nb} \rightarrow NH_3$$

$$\Delta G_{II} = (\mu_{NH_3} - \mu^\circ_{NH_3}) - (\mu_{[N]_{Nb}^{Sat}} - \tfrac{1}{2}\mu_{N_2}) - (3\mu_{[H]_{Nb}} - \tfrac{3}{2}\mu^\circ_{H_2})$$

$$+ (\mu^\circ_{NH_3} - \tfrac{1}{2}\mu^\circ_{N_2} - \tfrac{3}{2}\mu^\circ_{H_2})$$

The last term in parentheses is for the standard reaction: $\frac{1}{2} N_2(g) + \frac{3}{2} H_2(g) \rightarrow NH_3(g)$ and the free energy of this standard reaction is given by Kubachewski and Evans[112] as $\Delta G^{\circ T} = -10{,}400 + 7.1T \log T + 3.79\,T$. Therefore

$$\Delta G_{II}(T) - \Delta G^\circ_T = RT \ln \frac{P_{NH_3}}{P_{N_2(Sat)}^{1/2} \cdot P_{H_2}^{3/2}} .$$

At equilibrium, $\Delta G_{II}(T) = 0$.

Therefore, $P_{NH_3} = P_{N_2(Sat)}^{1/2} \cdot P_{H_2}^{3/2} \exp[-7.3]$

$$= P_{N_2(Sat)}^{1/2} \cdot P_{H_2}^{3/2} (6.8 \times 10^{-4})$$

Values of $P_{N_2(Sat,1000°K)}$ for niobium, tantalum and chromium are of the order 10^{-6} torr or less[95] and it seems reasonable to expect similar values for molybdenum and vanadium. Thus,

$$P_{NH_3}\ (1000°K) \approx 10^{-3} \cdot P_{H_2}^{3/2}\ (6.8 \times 10^{-4})$$

$$\approx 6.8 \times 10^{-7}\ (P_{H_2}^{3/2})$$

Since $P_{H_2} \approx 10^{-6} - 10^{-3}$ torr it is evident that the NH_3 pressures will be much too low to cause internal rupturing of the material if hydrogen pressures are in the range 10^{-6} to 10^{-3} torr. Similar conclusions hold for the reaction of hydrogen with carbon and oxygen in these first wall candidate materials.

IV-5. Effects of Hydrogen on Creep Resistance

There is a meagre evidence that the presence of hydrogen accelerates creep. For example, Douglas[113] found that the creep strength of Inconel was less in hydrogen than in argon at 704 and 815°C. McCoy[114] observed inferior creep resistance of Inconel, Nickel 200, Nickel 270, electron-beam zone-refined nickel and high purity copper in hydrogen. In all cases the minimum creep rate was greater and the rupture life shorter in hydrogen. However, the rupture ductility was not influenced by the hydrogen environment. Of more direct relation to CTR materials is the observation of McCoy and Douglas[115] that the creep rate of niobium at 3500 psi and about 980°C was greatly accelerated by moist or dry hydrogen flowing at 0.2 cfh as shown in Fig. 22.

Insufficient information is available to predict what the hydrogen pressure dependence of the creep behavior of these materials might be.

There is no established mechanism to explain this creep acceleration. It may be due to a hydrogen-impurity interaction which weakens the grain boundaries or hydrogen reduction of strengthening surface oxide films. Either rationalization is strictly conjecture at this point. Clearly, the above results require that hydrogen-environment accelerated creep must be reckoned with for stability of the CTR first wall structure.

IV-6. Hydrogen Environment Accelerated Crack Propagation

This potential phenomenon, illustrated schematically in Fig. 23, may well be more important at low temperatures but since it is possible at CTR operating temperatures, it is mentioned here. Any microscopic crack under tensile loading in the first wall will be exposed, on the plasma side, to deuterium and tritium. The coolant side will be exposed to liquid lithium containing tritium.

Recent work of Williams and Nelson[116] on steel provides some insight to this potential problem. They have demonstrated that the crack growth rate of steels in a molecular hydrogen gas environment is proportional to the hydrogen pressure to positive powers from 0.5 to 1.5. Furthermore, they demonstrated that the crack growth rate decreased with increasing temperature above approximately room temperature in a molecular hydrogen atmosphere. However, they showed subsequently[117] that the crack growth rate

increased with increasing temperature in the presence of a partially dissociated hydrogen environment at a molecular hydrogen pressure of 8×10^{-3} torr.

Since their work on steel covered a relatively low temperature range (up to 160°C) and pressures only down to 8×10^{-3} torr, it is difficult to predict how the hydrogen environment under CTR conditions would effect crack growth rate of the wall material. They have developed a theory which would enable a prediction of the crack growth rate under CTR conditions providing certain surface adsorption data are available. The necessary data are the surface atom migration energy and the heat of adsorption of hydrogen on the material in question.

Their observation that dissociated hydrogen gas produced enhanced crack growth rates may be especially relevant to the CTR situation where tritium in the liquid lithium blanket might be atomic. Combining the effects of liquid metal penetration into latent cracks with the atomic tritium could provide the condition for enhanced crack growth which would lead to premature rupture of the wall. Clearly, this is an area that needs attention.

IV-7. Interaction with Radiation-Produced Defects

Hydrogen atoms in the first wall may interact with radiation-produced point defects and helium atoms. The type of interaction envisioned are combinations such as H-He, H-vacancy, H-interstialcy or clusters of these. The effect that these combinations might have on the properties of the first wall material is

difficult to predict. Although the binding energies for the postulated interactions are unknown, it seems rather remote that they would be of sufficient magnitude at CTR temperatures. This is an area that should be investigated.

Even in the absence of any effects resulting from interactions of hydrogen atoms with other radiation-produced defects, voids created by vacancy combinations or helium bubbles could act as sites for hydrogen trapping which could then produce fissures on the type of spalling mentioned above.

IV-8. Helium Generation from Tritium Decay

Wall material can act as a source of helium which can itself lead to embrittlement[118,119]. This comes about as pointed out by Green[120], from the 12-year half-life radioactive decay of tritium according to $H^3 \rightarrow He^3 + \beta$. Clearly the amount of helium generated in this way will depend on the concentration of tritium in the wall material. A typical helium generation rate from (n,α) reactions in the wall would be about 0.02 atom percent per year from the CTR neutron flux. To develop an equivalent quantity of helium by tritium decay would require a steady tritium concentration of about 0.48 atom percent in the wall material (~40-80 ppmw depending on the wall material). As shown in Figs. 6-12 this concentration may be in the solubility range of the wall materials under CTR operating conditions. Thus, the possibility exists for tritium to enhance helium bubbles or embrittlement in the CTR structural material.

IV-9. Plasma Contamination or Poisoning

Whether plasma contamination by hydrogen isotopes is a real problem is uncertain to the author. The diffusion of protons back into the plasma region may constitute a poisoning action but the source of protons is only from (n,p) reactions and the quantity of protons developed in this manner is small, as indicated earlier. Since deuterium and tritium atoms escaping the plasma will be present in any event it would seem that back diffusion of deuterium and tritium would not be contaminating. Although there is no available evaluation of the effect of hydrogen isotopes diffusing back into the plasma zone, it is appropriate to recognize that this might occur to a significant degree.

If these hydrogen isotopes constitute a contaminant of the plasma, it appears that the permeation rate of tritium from the blanket will be the prime source of contamination. The permeation rate will depend on whether the transport of tritium is dependent on surface reactions or on bulk transport. Surface reaction control will depend on too many factors to be able to anticipate the magnitude of the rate. Experimental information is sorely needed here.

On the other hand, if bulk transport controls permeation, then the solubility of hydrogen isotopes and their diffusivity will be the important factors. The solubility, neglecting the (n,p) generated protons and the tritium and deuterium injected from the plasma, will depend on the hydrogen pressures surround-

ing the wall. This follows from Fick's first law for one dimensional planar diffusion:

$$J = -D\frac{\delta C}{\delta X}$$

where $$\frac{\delta C}{\delta X} = \frac{K(P_2^{1/2} - P_1^{1/2})}{d}$$

or $$J = \frac{-DK(P_2^{1/2} - P_1^{1/2})}{d}$$

Where J = flux or quantity of gas atoms per unit time passing unit area in units of micron liters per cm^2 per sec,

D = diffusivity of gas atoms in wall material,

$$D = D_o \exp\left[\frac{-\Delta H_{diffusion}}{RT}\right]$$

P_2 = hydrogen isotope pressure on the blanket side of the wall,

P_1 = hydrogen isotope pressure on plasma side of the wall,

d = wall thickness,

K = solubility coefficient: $K = K_o \exp\left[\frac{-\Delta H \text{ solution}}{RT}\right]$

Thus, it is evident that the permeability will depend on the pressures existing on either side of the wall. As mentioned earlier, these are not known presently but could both be in the range 10^{-6} to 10^{-3} or 10^{-2} torr.

Furthermore, it can be seen that the permeability increases as temperature is raised and as the heats of solution and diffusion decrease. On the other hand, as mentioned earlier, surface reactions may control and the above comments about permeation related to bulk diffusion become meaningless.

SUMMARY

The sources of hydrogen isotopes available to the CTR first wall are: (a) tritium from breeding reactions in the lithium blanket with an anticipated partial pressure of 10^{-6} to 10^{-3} torr depending on the tritium inventory selected; (b) tritium and deuterium at pressures ranging from 10^{-6} to 10^{-2} torr on the "vacuum" side of the wall; (c) injected energetic neutral tritons and deuterons escaping the plasma; (d) protons generated by (n,p) reactions in the wall. Of these sources, the injected energetic neutrals and the (n,p) reaction generated protons would appear, under normal conditions, not to contribute a significant quantity of hydrogen isotopes to the first wall. However, during CTR operations other point defects such as helium atoms and vacancies are produced in the wall and these may have a profound effect on the hydrogen isotope - wall material thermodynamics. While calculations based on a wall material containing only hydrogen isotopes suggest that the quantities of injected neutrals and (n,p) protons would be insignificant, the observation of hydrogen blisters indicates that very effective trapping sites or surface effects control the emission of the isotopes from the wall. Since little is known about the effectiveness of helium atoms and vacancies or clusters of them to trap hydrogen isotopes in the CTR operating range it is imperative that work be done in this area before it is possible to predict the steady-state distribution from the two sources just mentioned.

Hydrogen embrittlement will be a problem if the tritium inventory in the blanket is maintained during cool down except for stable austenitic stainless steel and molybdenum. Internal hydriding and reaction of hydrogen with other impurities such as oxygen, nitrogen and carbon seem to be rather innocuous under the conditions expected. Additional work is required before the effect of hydrogen on the creep resistance of potential first wall materials can be assessed accurately. This is also the situation regarding hydrogen environment accelerated crack propagation under CTR conditions, particularly since the hydrogen is dissolved in liquid lithium.

The generation of helium by tritium decay in the wall material and plasma poisoning due to hydrogen isotope emission from the wall will depend on the actual tritium inventory in the blanket and the gas pressure on the "vacuum" side. A factor of ignorance here is the equilibrium partial pressures of hydrogen or tritium over the lithium blanket under CTR conditions.

ACKNOWLEDGEMENT

The author gratefully acknowledges the comments and advice of friend and colleague, Dr. J. W. Patterson.

Table I. Hydrogen Concentration to 1000Å Depth Due to Energetic D or T

Metal	Atomic Vol. ($\frac{cc}{atom}$)	Atoms in cm^2 x 1000Å (M)	$\lvert H/M \rvert$ sec.$^{-1}$ 10^{14} cm^{-2}-sec.$^{-1}$	10^{16} cm^{-2}-sec.$^{-1}$
Vanadium	1.39×10^{-23}	7.21×10^{17}	1.4×10^{-4}	1.4×10^{-2}
Molybdenum	1.56 "	6.41 "	1.5 "	1.6 "
Niobium	1.79 "	5.58 "	1.8 "	1.8 "
Austenitic Stainless	1.16 "	8.61 "	1.2 "	1.2 "
Titanium	1.76 "	5.67 "	1.8 "	1.8 "
Yttrium	3.30 "	3.03 "	3.3 "	3.3 "
Zirconium	2.33 "	4.28 "	2.3 "	2.3 "

Table II. Proton Production Rate and Maximum Concentration from (n,p) Reactions

Metal	$\sigma(n,p)^+$ barns	$\dot{R}$, sec.$^{-1}$	C_{max} ++
Vanadium	0.036	3.6×10^{-11}	0.007×10^{-6}
Molybdenum	0.120	12.0×10^{-11}	3.75 "
Niobium	0.022	2.2×10^{-11}	0.005 "
Austenitic Stainless	0.151	15.1×10^{-11}	0.189 "
Titanium	0.091	9.1×10^{-11}	0.284 "
Yttrium	0.023	2.3×10^{-11}	0.072 "
Zirconium	0.025	2.5×10^{-11}	0.078 "

+ For 14 MeV neutrons

++ At steady-state assuming C_1 and C_o are zero.

REFERENCES

1. W. C. Gough and B. J. Eastlund: "The Prospects of Fusion Power," Sci. Am., v. 224, 1971, p. 50.
2. H. Postma: "Engineering and Environmental Aspects of Fusion Power Reactors," Nuclear News, v. 14, 1971, p. 57.
3. D. Steiner: "Neutron Irradiation Effects and Tritium Inventories Associated with Alternate Fuel Cycles for Fusion Reactors," Nuclear Fusion, v. 11, 1971, p. 305.
4. A. P. Fraas: "A Diffusion Process for Removing Tritium from the Blanket of a Thermonuclear Reactor," ORNL-TM-2358, Dec. 1968.
5. A. P. Fraas and H. Postma: "Preliminary Appraisal of the Hazards Problems of a D-T Fusion Reactor Power Plant," ORNL-TM-2822, Nov. 1970.
6. D. Steiner and A. P. Fraas: "Preliminary Observations on the Radiological Implications of Fusion Power," Nuclear Safety, to be published.
7. C. E. Messer: "A Survey Report on Lithium Hydride," USAEC Report No. NYO-9470, Oct. 27, 1970, Tufts University, Medford 55, Massachusetts.
8. F. K. Heumann and O. N. Salmon: "The Lithium Hydride, Deuteride and Tritide Systems," USAEC Rept. No. KAPL-1667, Dec. 1, 1956, Knolls Atomic Power Laboratory, Schnectady, New York.

9. D. Steiner: "Tokamak Fusion Reactor," Fusion Reactor First Wall Materials Meeting AEC-Germantown, USAEC Rept. No. WASH 1206 ed. by L. C. Ianniello, p. 1, April 1972, Washington, D.C.

10. Task Group: "Surface Effects," Fusion Reactor First Wall Materials Meeting AEC-Germantown, USAEC Rept. No. WASH 1206, ed. by L. C. Ianniello, p. 79, April 1972, Washington, D.C.

11. G. M. McCracken: Proceedings of the International Working Sessions on Fusion Reactor Technology, Oak Ridge National Laboratory, USAEC Rept. No. CONF-710624, p. 124, Oak Ridge, Tennessee.

12. D. Steiner: "The Nuclear Performance of Fusion Reactor Blankets," Nucl. Appl. Tech., v. 9, 1970, p. 83.

13. M. D. Goldberg, S. F. Mughabghab, B. A. Magurno and V. M. May: "Neutron Cross Sections," Sigma Center, Brookhaven National Laboratory Report No. BNL 325, 1966.

14. E. Veleckis and R. K. Edwards: Jnl. Phys. Chem., v. 73, 1969, p. 683-692.

15. L. Johnson, M. J. Dresser and E. E. Donaldson: "Adsorption and Absorption of Hydrogen by Niobium," Report No. RLO-2221-T-7-3, Washington State University, Pullman, Washington 99163.

16. A. Sieverts and K. Bruning: Arch. Eisenhuttenwesen, v. 7, 1933-34, p. 641.

17. W. Oates and Rex B. McLellan: Scripta Met., v. 6, 1972, p. 349-352.

18. M. L. Hill: Jnl. Metals, v. 12, 1960, p. 725.

19. P. M. S. Jones, R. Gibson and J. A. Evans: "The Permeation and Diffusion of Hydrogen in Molybdenum," AWRE Rept. No. O-16/66, Aldermaston, Berkshire, England, February 1966.

20. M. H. Armbruster: Jnl. Am. Chem. Soc., v. 65, 1943, p. 1043.

21. R. L. Beck and W. M. Mueller: Metal Hydrides ed. by W. M. Mueller, J. P. Blackledge and G. G. Libowitz, Academic Press, N. Y., 1968, p. 241.

22. R. L. Beck: "Research and Development of Metal Hydrides," USAEC Rept. LAR-10, Denver Research Institute, Denver, Colorado, Nov. 1960.

23. L. N. Yannopoulos, R. K. Edwards and P. G. Wahlbeck: Jnl. Phys. Chem., v. 69, 1965, p. 2510.

24. W. Geller and T. Sun: Arch. Eisenhuttenwesen, v. 21, 1950, p. 423-430.

25. J. H. Austin and T. S. Elleman: Jnl. Nuclear Matls. v. 43, 1972, p. 119-126.

26. J. Völkl, G. Schaumann and G. Alefeld: Jnl. Phys. Chem. Solids, v. 31, 1970, p. 1805-1809.

27. M. W. Mallett and W. M. Albrecht: Jnl. Electrochem. Soc., v. 104, 1957, p. 142-146.

28. V. L. Gelezumas, P. K. Conn and R. H. Price: Jnl. Electrochem. Soc., v. 110, 1963, p. 799-805.

29. R. J. Wasilewski and G. L. Kehl: Metallurgica, v. 50, 1954, p. 255-230.

30. B. W. Roberts and H. C. Rogers: Trans. AIME, 206, 1956, p. 1213-1215.

31. A. W. Magnusson and W. M. Baldwin, Jr.: J. Mech and Phys. Solids, v. 5, 1957, p. 172.

32. B. A. Loomis and O. N. Carlson: Proc. Third Annual Reactor Metals Conf. AIME, vol. 2, Interscience, N. Y., 1959, p. 227.

33. A. L. Eustice and O. N. Carlson: Trans. AIME, v. 221, 1961, p. 238-241.

34. R. H. Van Fossen, Jr., T. E. Scott and O. N. Carlson: J. Less-Common Metals, v. 9, 1965, p. 437-451.

35. D. H. Sherman, C. V. Owen and T. E. Scott: Trans. TMS AIME, v. 242, 1968, p. 1775-1784.

36. C. V. Owen and T. E. Scott: Met. Trans., v. 3, 1972, p. 1715.

37. C. J. McHargue and H. E. McCoy: Trans. AIME, v. 227, 1963, p. 1170.

38. A. L. Eustice and O. N. Carlson: Trans. ASM, v. 53, 1961, p. 501.

39. T. W. Wood and R. D. Daniels: Trans. AIME, v. 233, 1965, p. 898-903.

40. B. A. Wilcox, A. W. Brisbane and R. F. Klinger: ASM Trans. Quart., v. 55, 1962, p. 179.

41. T. G. Oakwood and R. D. Daniels: Trans. TMS AIME, v. 242, 1968, p. 1327.

42. B. Longson: "The Hydrogen Embrittlement of Niobium," TRG-Report - 1035(c) Jan. 1966.

43. D. G. Westlake: Trans. TMS AIME, v. 245, 1969, p. 1969-1973.

44. W. T. Chandler and R. J. Walter: Refractory Metal Alloys (Metallurgy and Technology) p. 197, ed. by I. Machlin, R. T. Begley and E. D. Weisert, Plenum Press, N. Y., 1968.

45. A. G. Ingram, E. S. Bartlett and H. R. Ogden: Trans. TMS AIME v. 227, 1963, p. 131.

46. B. A. Wilcox and R. A. Huggins: Columbium Metallurgy ed. by D. L. Douglass and F. W. Kunz, Interscience Pub., N. Y., 1961, p. 257.

47. Y. Sasaki and M. Amano: Trans. Japan Inst. of Metals, v. 10, 1969, p. 26.

48. A. J. Maeland: Jnl. Phys. Chem., v. 68, 1964, p. 2197-2200.

49. R. J. Walter and W. T. Chandler: Trans. TMS-AIME, v. 233, 1965, p. 762-765.

50. A. Lawley, W. Liebmann and R. Madden: Acta Met., v. 9, #9 1961, p. 841-850.

51. F. Feuerstein: Effects of Space Environment on Materials, Proc. of Nat'l Symp. of Soc. of Aerospace Material and Process Engineers, St. Louis, Mo., April 19-21, 1967, p. 299.

52. J. D. Hobson and J. Hewett: Jnl. I. and S. Inst., v. 173, 1953, p. 313-340.

53. R. M. Vennett and G. S. Ansell: Trans. Quart. ASM, v. 62, 1969, p. 1007-1013.

54. F. Eisenkolb and G. Ehrlich: Arch. f.d. Eisenhuttenwesen, v. 25, 1954, p. 187-194.

55. C. Sykes, H. H. Burton and C. C. Gegg: Jnl. J. and S. Inst., v. 156, 1947, p. 155-180.

56. H. C. Van Ness: Petroleum Refiner, v. 35, 1956, p. 160-163.

57. H. C. Van Ness and B. F. Dodge: Chem. Engrng. Progress, v. 51, 1955, p. 266-271.

58. E. R. Slaughter: Jnl. of Metals, v. 8, 1956, p. 430-431.

59. C. A. Zapffe and M. E. Haslem: Trans. AIME, v. 167, 1946. p. 281-308.

60. R. L. Mills and F. J. Edeskuty: Chem. Eng. Progress, v. 52, 1956, p. 477.

61. I. Matsushima, D. Deegan and H. H. Uhlig: Corrosion v. 21, 1965, p. 23.

62. P. Blanchard and A. R. Troiano: Revue de Met., v. 57, 1969, p. 409.

63. M. B. Whiteman and A. R. Troiano: Corrosion, v. 21, 1965, p. 53.

64. R. M. Vennett and G. S. Ansell: Trans. ASM, v. 60, 1967, p. 242.

65. R. B. Benson, Jr., R. K. Dann and L. W. Roberts, Jr.: Trans. TMS-AIME, v. 242, 1968, p. 2199-2205.

66. M. L. Holzworth: Corrosion, v. 25, 1969, p. 107-115.

67. R. Lagneborg: J. Iron Steel Inst., v. 207, 1969, p. 363-366.

68. Ye. P. Nechai and K. V. Popov: Phys. of Metals and Metallography, v. 11(2), 1961, p. 70-74.

69. C. M. Craighead, G. A. Lenning and R. I. Jaffee: Trans. AIME, v. 206, 1956, p. 923.

70. A. R. Troiano: 1959 Edward De Mille Campbell, Memorial Lecture, Trans. ASM, v. 52, 1960, p. 54.

71. P. Cotterill: Progress Mater. Sci., v. 9 (4), 1961.

72. M. R. Louthan: Trans. AIME, v. 227, 1963, p. 1166.

73. D. N. Williams, F. R. Schwartzberg and R. I. Jaffee: Trans. ASM, v. 52, 1960, p. 182.

74. D. N. Williams, F. R. Schwartzberg and R. I. Jaffee: Trans. ASM, v. 51, 1959, p. 802.

75. R. I. Jaffee and D. N. Williams: Trans. ASM, v. 51, 1959, p. 820.

76. D. N. Williams and R. I. Jaffee: Jnl. Less-Common Metals, v. 2, 1960, p. 42.

77. D. N. Williams: Jnl. Inst. of Metals, v. 91, 1962/63, p. 147-152.

78. R. D. Daniels, R. J. Quigg and A. R. Troiano: Trans. ASM, v. 51, 1959, p. 843.

79. C. J. Beevers, M. R. Warren and D. V. Edmonds: Jnl. Less-Common Metals, v. 14, 1968, p. 387-396.

80. D. G. Westlake: ASM Trans. Qtrly. v. 56, 1963, p. 1.

81. D. Weinstein and F. C. Holtz: ASM Trans. Qtrly., v. 57, 1964, p. 284.

82. M. R. Louthan: ASM Trans. Qtrly., v. 57, 1964, p. 1004.

83. R. P. Marshall and M. R. Louthan: ASM Trans. Qtrly., v. 56, 1963, p. 693.

84. D. G. Westlake: Trans. TMS-AIME, v. 233, 1965, p. 368.

85. C. E. Coleman and D. Hardie: Jnl. Less-Common Metals, v. 11, 1966, p. 168-185.

86. C. D. Fearnehough and A. Cowan: Jnl. Nucl. Mater., v. 22, 1967, p. 137.

87. M. R. Warren and C. J. Beevers: Jnl. Nucl. Mater., v. 26, 1968, p. 273-285.

88. G. A. Nelson and R. T. Effinger: Welding Jnl. Res. Supp., v. 34, 1955, p. 12-15.

89. A. S. Tetelman and W. D. Robertson: Trans. AIME, v. 224, 1962, p. 775.

90. A. S. Tetelman and W. D. Robertson: Acta Met., v. 11, 1963, p. 415.

91. F. deKazinczy: Jernkontorets Annaler, v. 140, 1956, p. 347-359.

92. J. Donhowe and G. L. Kulcinski: Radiation Blistering, Fusion Reactor First Wall Materials Meeting AEC-Germantown, USAEC Rept. No. WASH 1206, ed. by L. C. Ianniello, p. 75, April 1972, Wash. D.C.

93. M. Kaminsky: talk presented in a special session on Design and Materials Problems in Thermonuclear Reactors at The TMS-AIME Spring May 1972 Meeting in Boston, Mass.

94. F. W. Wiffen: to be published in Proceedings of International Conference on Radiation-Induced Voids in Metals, held in Albany, New York, June 9-11, 1971.

95. J. D. Fast: Interaction of Metals and Gases, Vol. 1, Academic Press, 1965, New York, p. 59 and p. 215.

96. G. G. Libowitz: The Solid State Chemistry of Binary Metal Hydrides, W. A. Benjamin, Inc., 1965, New York, p. 66.

97. H. J. Goldschmidt: Interstitial Alloys, Plenum Press, 1967, New York, p. 463.

98. H. C. Rogers: Chapter 9, Fracture of Engineering Materials ASM, 1964, p. 163.

99. F. N. Rhines and W. A. Anderson: Trans. AIME, v. 143, 1941, p. 312-325.

100. C. E. Ransley: Jnl. Inst. Metals, v. 65, 1939, p. 147.

101. E. Mattsson and F. Schuckher: Jnl. Inst. of Metals, v. 87, 1958, p. 241-247.

102. S. Harper, V. A. Callcut, D. W. Townsend and R. Everall: Jnl. Inst. Metals, v. 90, 1962, p. 414 and p. 423.

103. J. D. Fast: Interaction of Metals and Gases, v. 1, Academic Press, New York, 1965, p. 54-57.

104. J. C. Chaston: Jnl. Inst. Metals, v. 71, 1945, p. 23-39.

105. D. L. Marten and E. R. Parker: Trans. AIME, v. 153, 1943, p. 237-244.

106. R. L. Klueh and W. W. Mullins: Trans. TMS-AIME, v. 242, 1968, p. 237-244.

107. R. E. Allen, R. J. Jansen, P. C. Rosenthal and V. H. Vitovec: Proc. Amer. Petroleum Inst., Sect. III, v. 41, 1961, p. 74-85.

108. R. E. Allen, P. J. Jansen, P. C. Rosenthal and F. H. Vitovec: Proc. Amer. Petroleum Inst., Sect. III, v. 42, 1962, p. 452-462.

109. F. H. Vitovec: Proc. Amer. Petroleum Inst., Sect. III, v. 44, 1964, p. 179-188.

110. J. K. Stanley: Trans. ASM, v. 44, 1952, p. 1097.

111. H. H. Podgurski: Trans. TMS-AIME, v. 221, 1961, p. 389-394.

112. O. Kubaschewski and E. LL. Evans: Metallurgical Thermochemistry, Pergamon Press, 1958, New York.

113. D. A. Douglas: High Temperature Materials, p. 429, ed. by R. F. Hehemann and G. M. Ault, John Wiley and Sons, New York 1959.

114. H. E. McCoy, Jr.: Effects of Hydrogen on the High Temperature Flow and Fracture Characteristics of Metals: Ph.D. Thesis, University of Tennessee, June 1964.

115. H. E. McCoy, Jr. and D. A. Douglas: Columbium Metallurgy, p. 85, ed by D. L. Douglass and F. W. Kunz, Interscience Publishers, New York, 1961.

116. D. D. Williams and H. G. Nelson: Met. Trans. v. 1, 1970, p. 63-68.

117. H. G. Nelson, D. P. Williams and A. S. Tetelman: Met. Trans., v. 2, 1971, p. 953.

118. D. Kramer, H. R. Brager, C. G. Rhodes and A. G. Pard: Jnl. Nucl. Mat., v. 25, 1968, p. 121-131.

119. D. Kramer, K. R. Garr, C. G. Rhodes and A. G. Pard: Jnl. Iron and Steel Inst., v. 207, 1969, p. 1141-1146.

120. W. V. Green: "Tritium Effects and Some Possible Fatigue Effects in Pulsed Reactors," Fusion Reactor First Wall Materials Meeting AEC-Germantown, USAEC Rept. No. WASH 1206, ed. by L. C. Ianniello, p. 57, April 1972, Washington, D.C.

FIGURE CAPTIONS

Fig. 1. A conceptual CTR core cross-section after Fraas and Postma[5].

Fig. 2. An enlarged view of the first wall region of the conceptual CTR core illustrated in Fig. 1 showing anticipated environmental conditions.

Fig. 3. A schematic illustration of the Li-LiH phase diagram after Messer[7]. The cross-hatched region at the upper left-hand side is an exaggerated indication of the CTR range.

Fig. 4. Some equilibrium pressure-temperature-composition plots for the Li-LiH system after Messer[7].

Fig. 5. A log-log plot of the 700°C data for Li-T and Li-H from Heumann and Salmon[8]. Actual data are indicated in the upper right-hand portion of the graph. Extrapolation to the anticipated CTR range of composition by extension of the data lines or by Sievert's Law ($\log p = 2 \log C$) is shown by dark or light lines respectively.

Fig. 6. Equilibrium pressure-temperature-composition data for the V-H system in the anticipated CTR temperature range. These curves are based on an extrapolation to lower pressures of data from Velickis and Edwards[14].

Fig. 7. Equilibrium pressure-temperature-composition data for the Nb-H system in the anticipated CTR temperature range. The upper set of curves are based on extrapolation of Veleckis and Edwards[14] data and the lower set are experimental data from Johnson et al.[15]

Fig. 8. Equilibrium pressure-temperature-composition data for the Mo-H system plotted on a log composition vs reciprocal absolute temperature scale to include the expected low pressure value. Data are from Sievert's and Bruning[16], and Oates and McLellan[17] and the small line from Hill's equation for the range studied[18]. The plots of Jones et al.[19] represent their equation at 760 torr and 10^{-6} torr hydrogen pressure.

Fig. 9. Equilibrium pressure-temperature-composition data[20] for 18 Cr-8 Ni austenitic stainless steel. The 900°C data were determined by extrapolation.

Fig. 10. Equilibrium pressure-temperature-composition data[21] for zirconium in the temperature range of interest.

Fig. 11. Equilibrium Pressure-temperature-composition data[22] for titanium in the temperature range of interest.

Fig. 12. Equilibrium pressure-temperature-composition data[23] for yttrium in the temperature range of interest.

Fig. 13. Diffusivities of hydrogen and its isotopes in the metals indicated. The hydrogen-stainless steel data are from Geller and Sun,[24] the tritium-stainless steel data from Austin and Elleman,[25] the molybdenum data from Jones et al.[19] and the niobium and vanadium data are from Völkl et al.[26]

Fig. 14. Diffusivities of hydrogen and its isotopes in the metals indicated. Data for α Zr are from Mallett and Albrecht[27], and for β Zr from Gelezumas et al.[28] while the data for titanium are from Wasilewski and Kehl[29].

Fig. 15. Schematic illustration of the ductility behavior of hydrogen charged metal depicting four temperature ranges, A,B,C and D, of special interest.

Fig. 16. Ductility of vanadium containing indicated concentrations of hydrogen vs. test temperature showing that the DBTT increases with hydrogen concentration. The cross-hatched region indicates the temperature range of visual observations of hydride formation on cooling.

Fig. 17. Relation between hydrogen content and the reciprocal of the DBTT for vanadium. The behavior of niobium is from Longson[42].

Fig. 18. Phase diagram for the vanadium-hydrogen system given by Maeland[48].

Fig. 19. Phase diagram for the niobium-hydrogen system given by Walter and Chandler[49].

Fig. 20. A schematic illustration of the blistering phenomenon due primarily to injected energetic deuterium and tritium atoms including the contributions from internal hydrogen.

Fig. 21. A schematic illustration of the physical processes of internal hydriding using dissolved titanium as the example.

Fig. 22. Experimental results from McCoy and Douglas[115] showing the effect of a hydrogen environment on creep of niobium.

Fig. 23. A schematic illustration of the physical process envisioned for hydrogen atmosphere accelerated crack propagation.

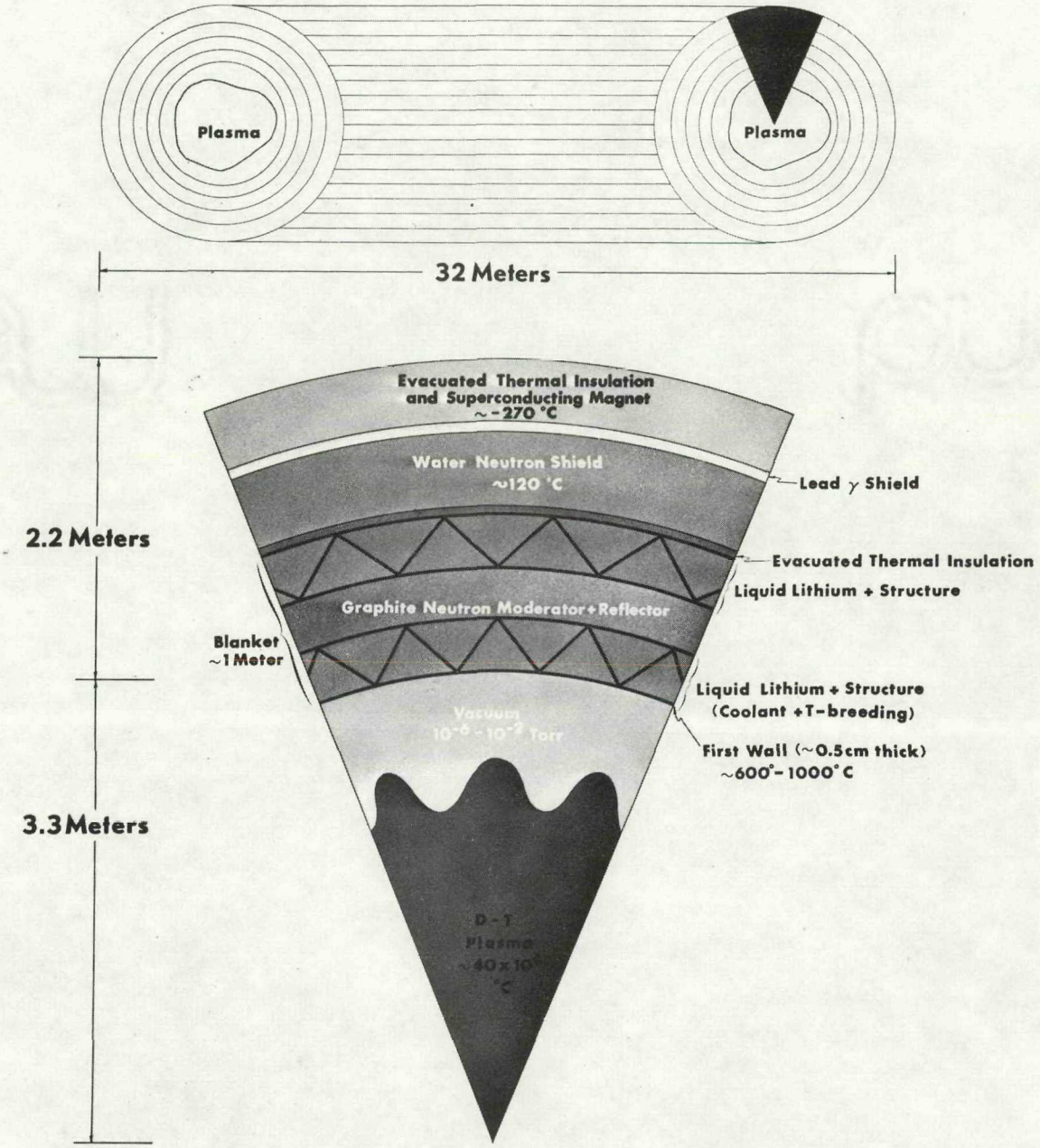

CROSS-SECTION OF A CONCEPTUAL CTR CORE DESIGN

Fig. 1. A conceptual CTR core cross-section after Fraas and Postma (5)

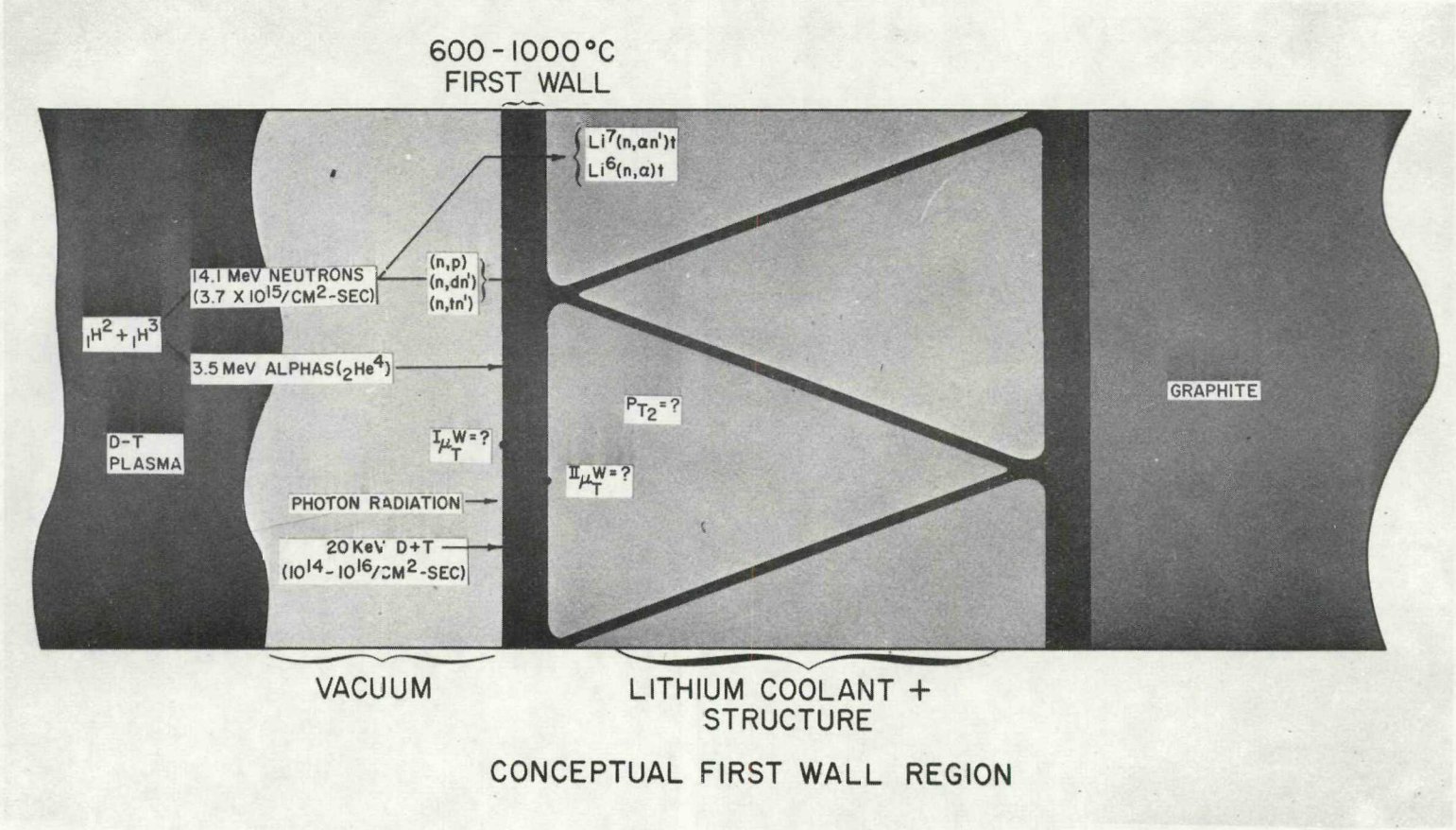

Fig. 2. An enlarged view of the first wall region of the conceptual CTR core illustrated in Figure 1 showing anticipated environmental conditions

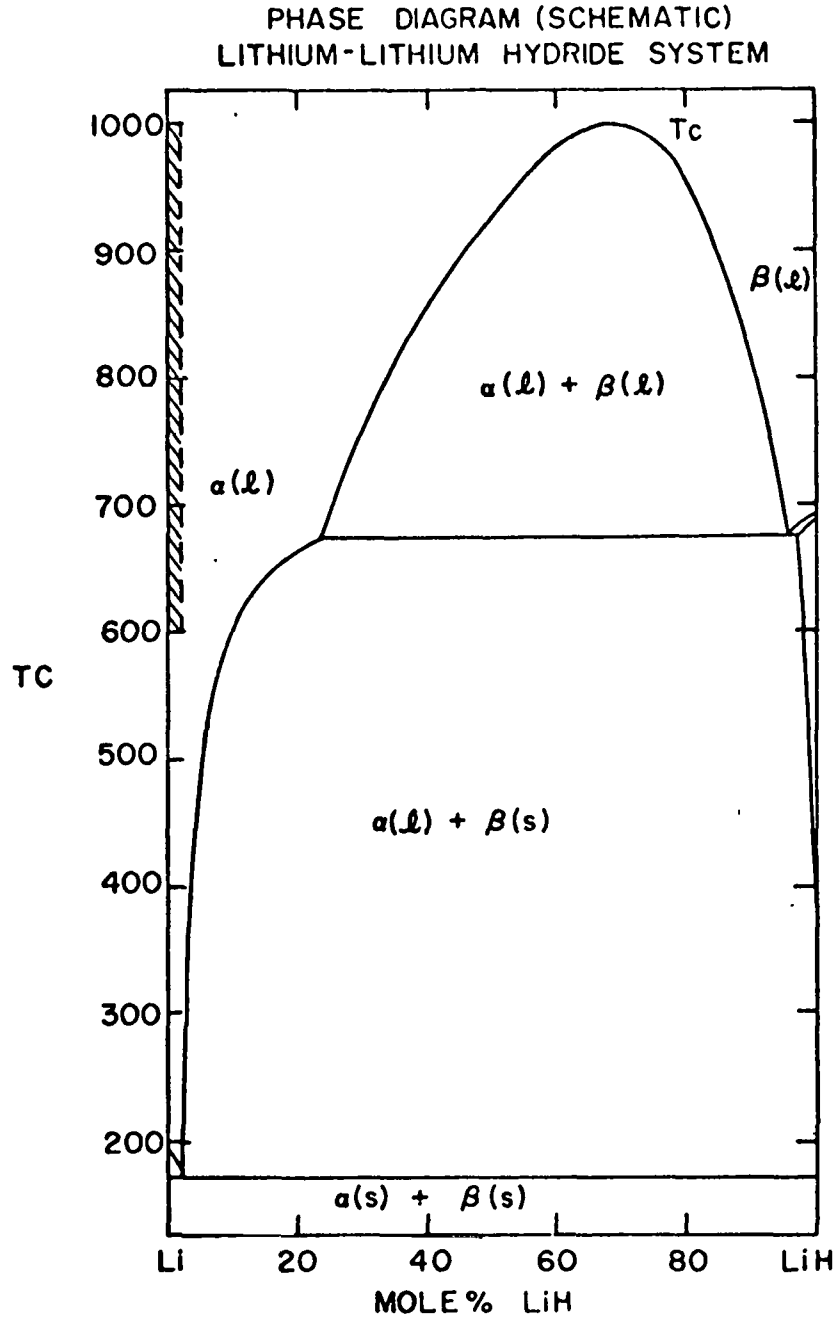

Fig. 3. A schematic illustration of the Li-LiH diagram after Messer[7]. The cross-hatched region at the upper left-hand side is an exaggerated indication of the CTR range.

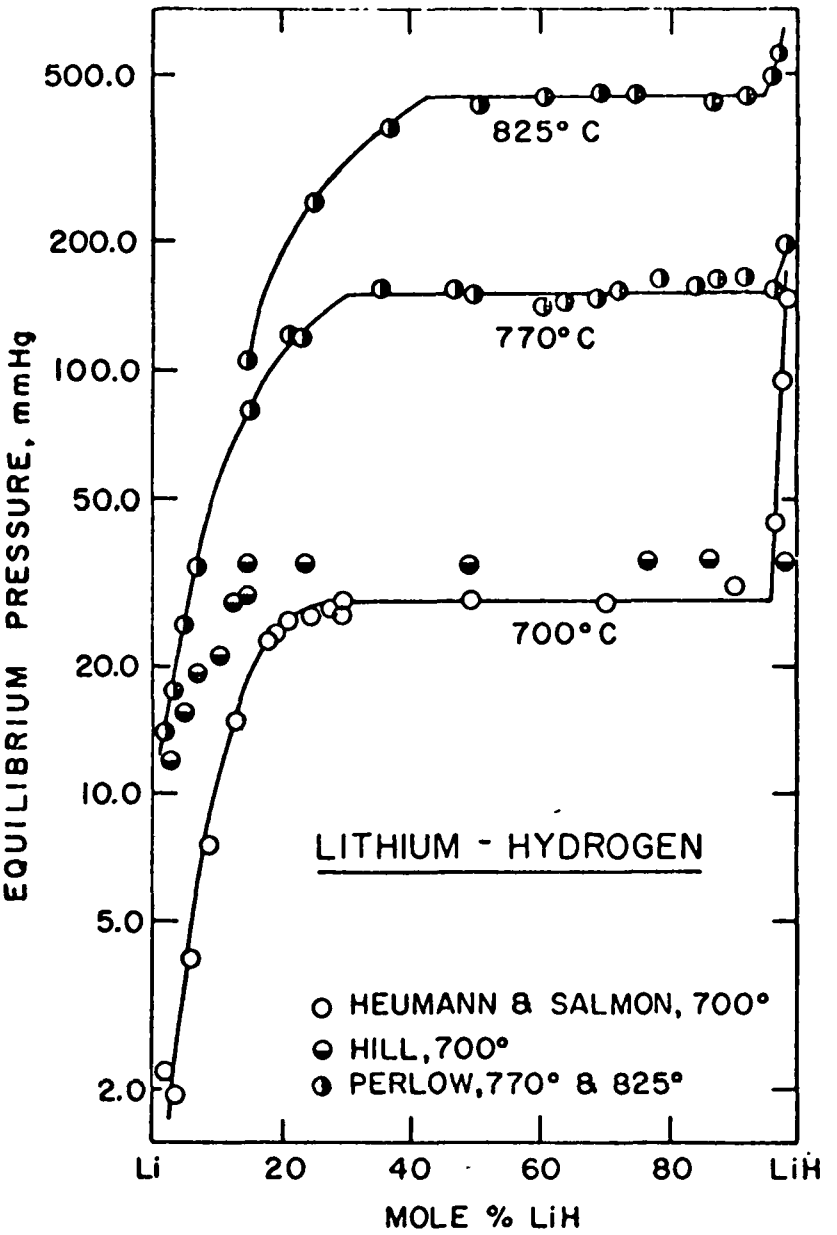

Fig. 4. Some equilibrium pressure-temperature-composition plots for the Li-LiH system after Messer[7].

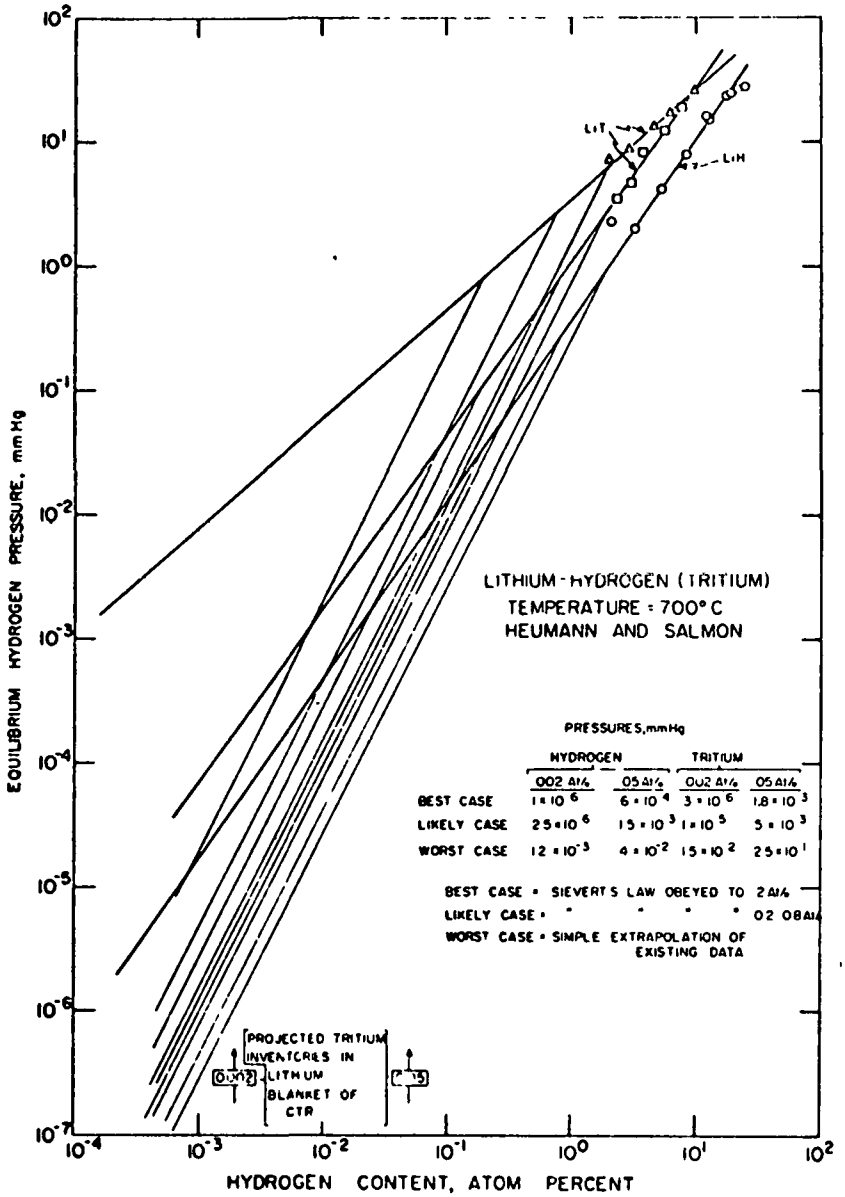

Fig. 5. A log-log plot of the 700°C data for Li-T and Li-H from Heumann and Salmon[8]. Actual data are indicated in the upper right-hand portion of the graph. Extrapolation to the anticipated CTR range of composition by extension of the data lines or by Sievert's Law (log p = 2 log C) is shown by dark or light lines respectively.

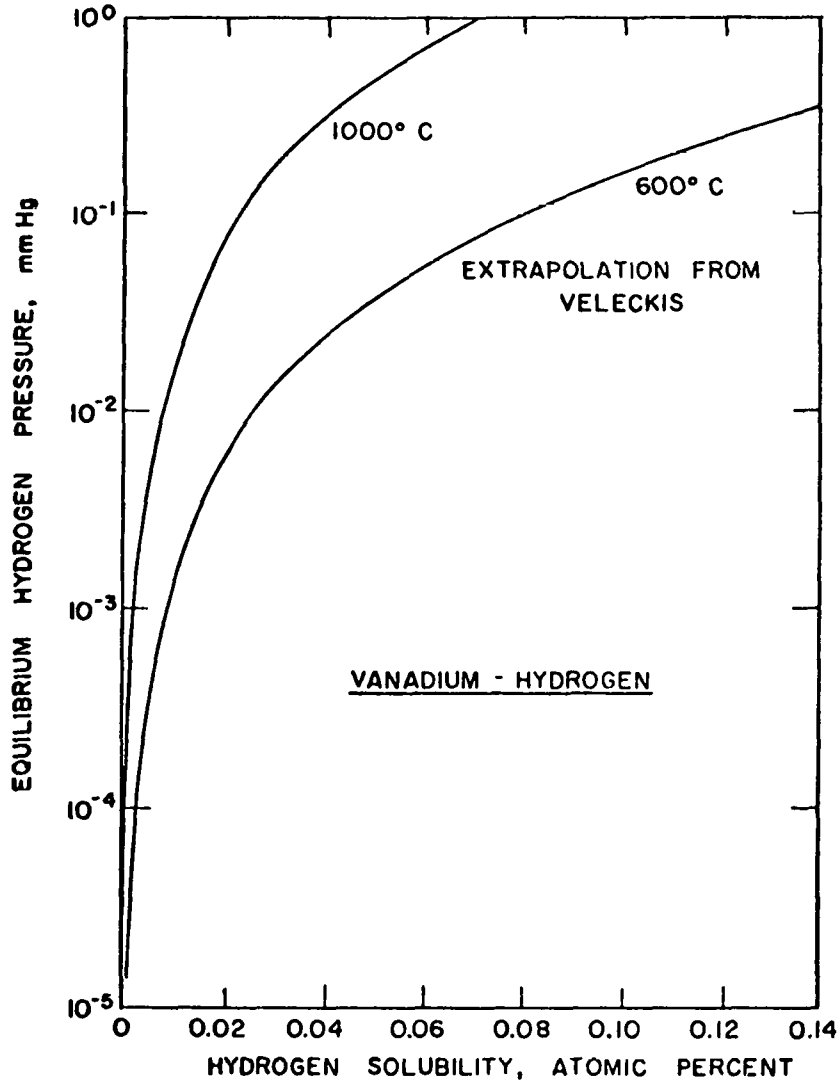

Fig. 6. Equilibrium pressure-temperature-composition data for the V-H system in the anticipated CTR temperature range. These curves are based on an extrapolation to lower pressures of data from Velickis and Edwards[14].

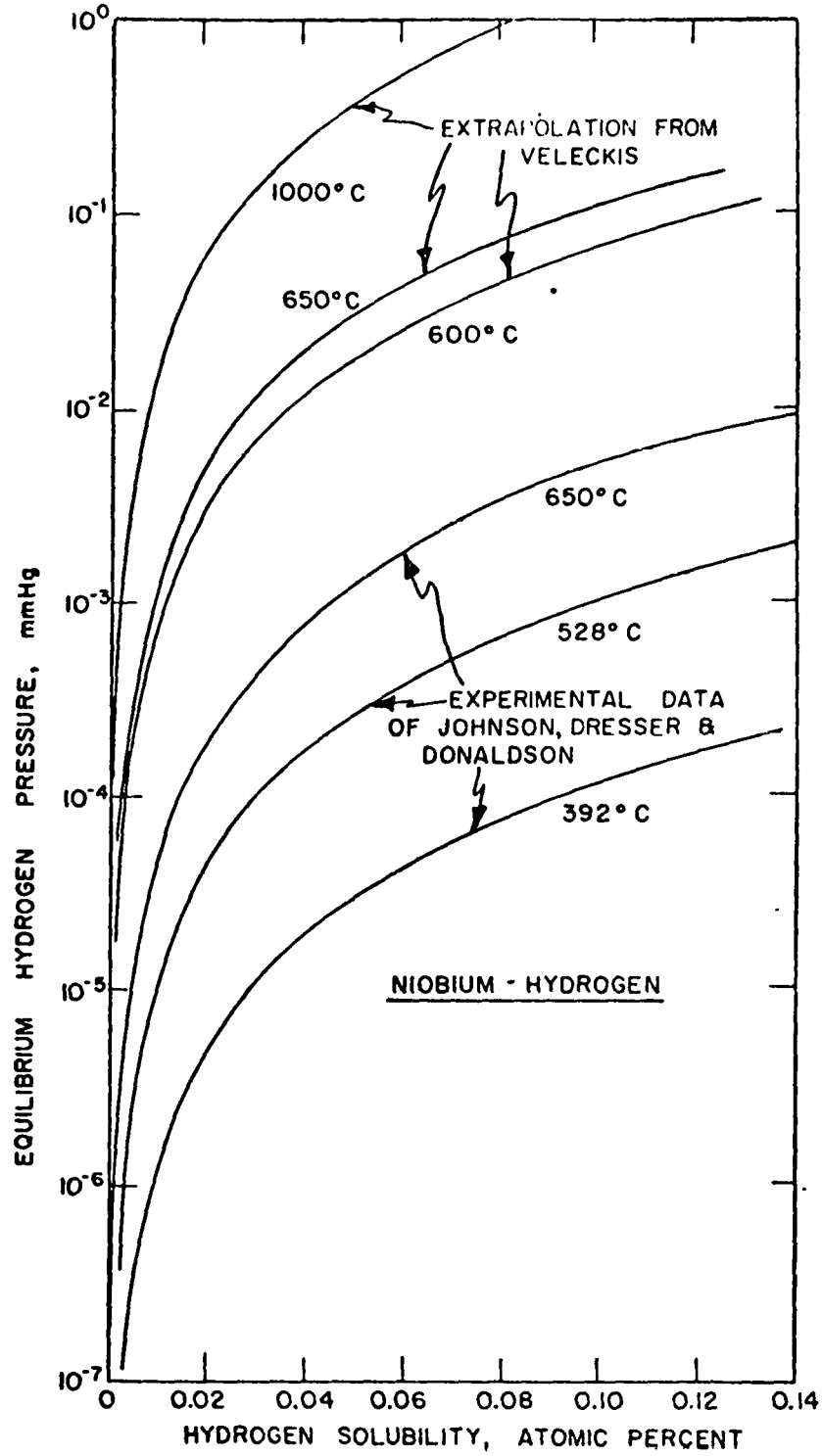

Fig. 7. Equilibrium pressure-temperature-composition data for the Nb-H system in the anticipated CTR temperature range. The upper set of curves are based on extrapolation of Velickis and Edwards[14] data and the lower set are experimental data from Johnson et al.[15]

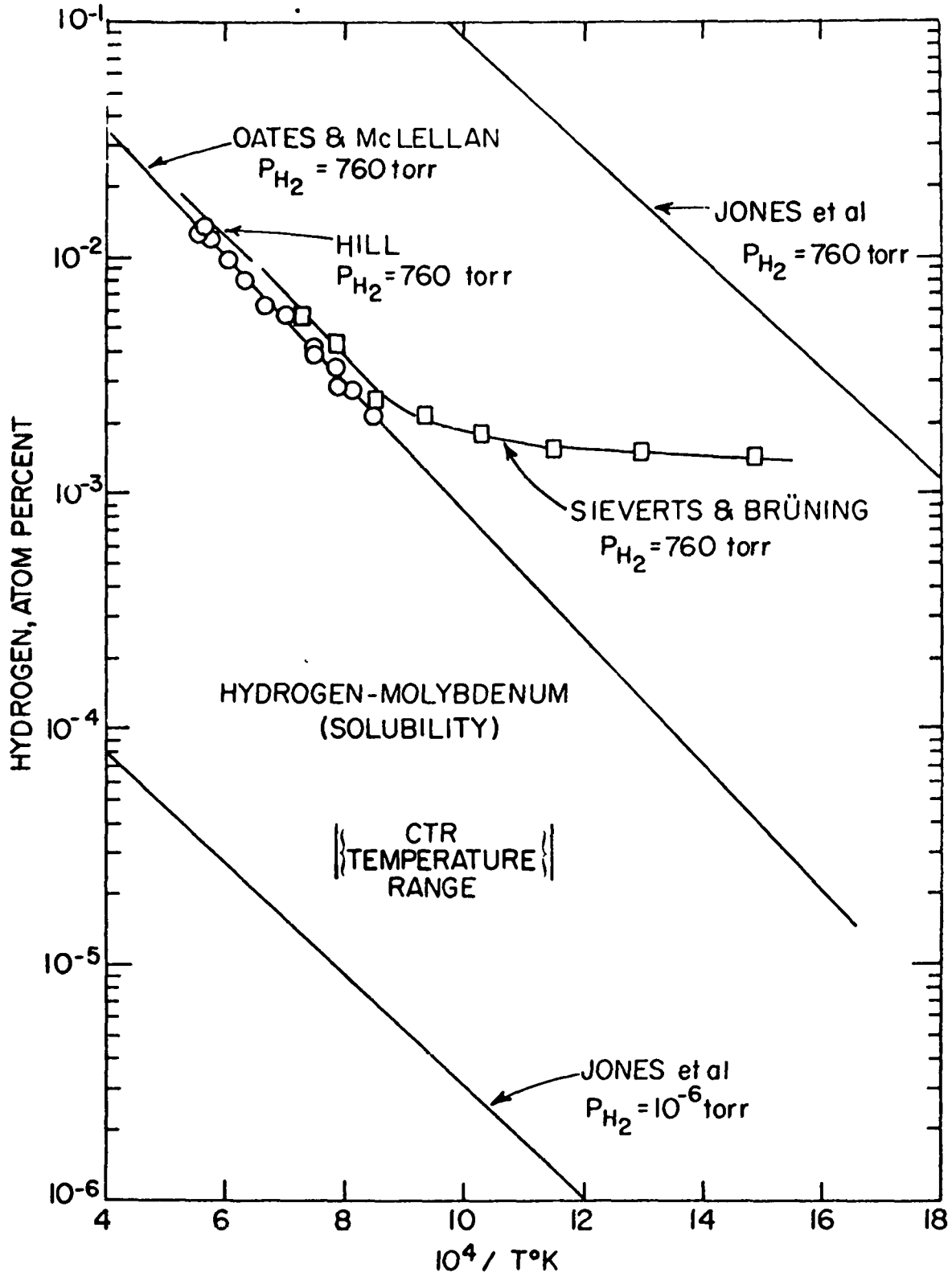

Fig. 8. Equilibrium pressure-temperature-composition data for the Mo-H system plotted on a log composition vs reciprocal absolute temperature scale to include the expected low pressure value. Data are from Sievert's and Bruning[16], and Oates and McLellan[17] and the small line from Hill's equation for the range studied[18]. The plots of Jones et al.[19] represent their equation at 760 torr and 10^{-6} torr hydrogen pressure.

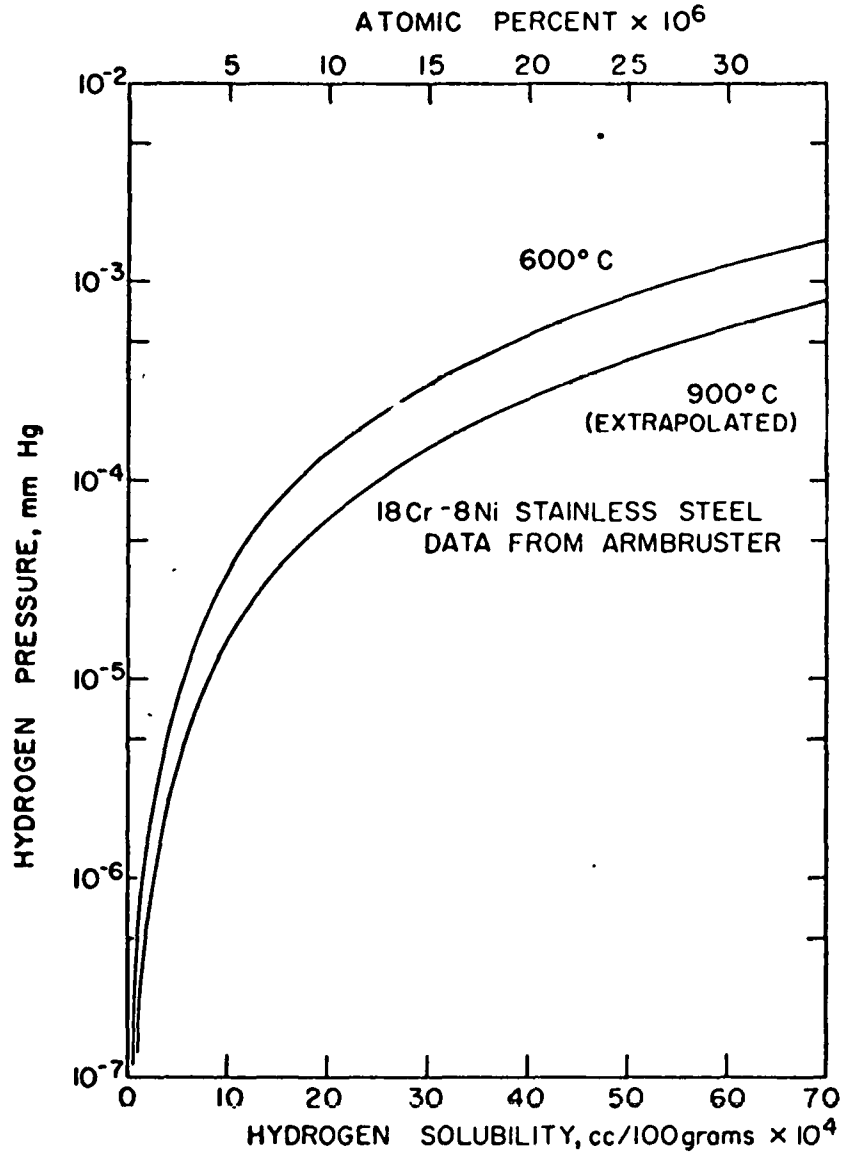

Fig. 9. Equilibrium pressure-temperature-composition data[20] for 18 Cr-8 Ni austenitic stainless steel. The 900°C data were determined by extrapolation.

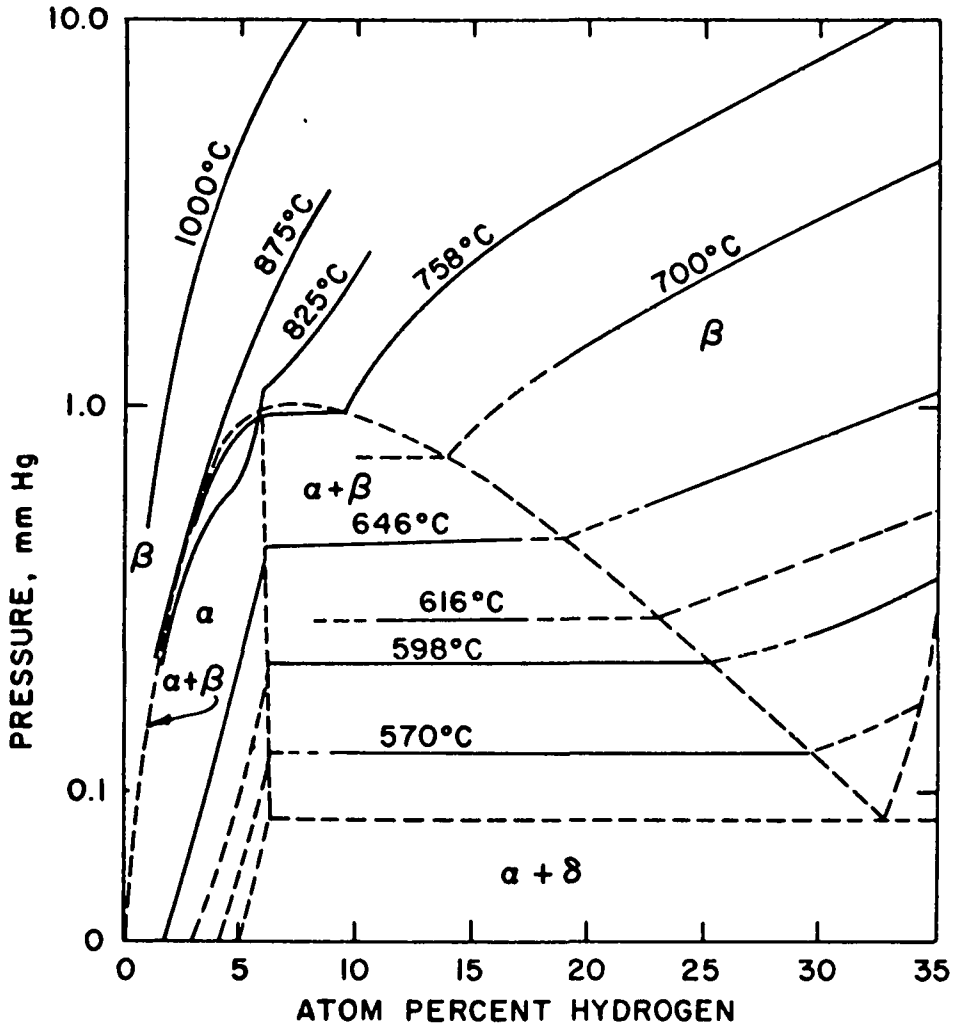

Fig. 10. Equilibrium pressure-temperature-composition data[21] for zirconium in the temperature range of interest.

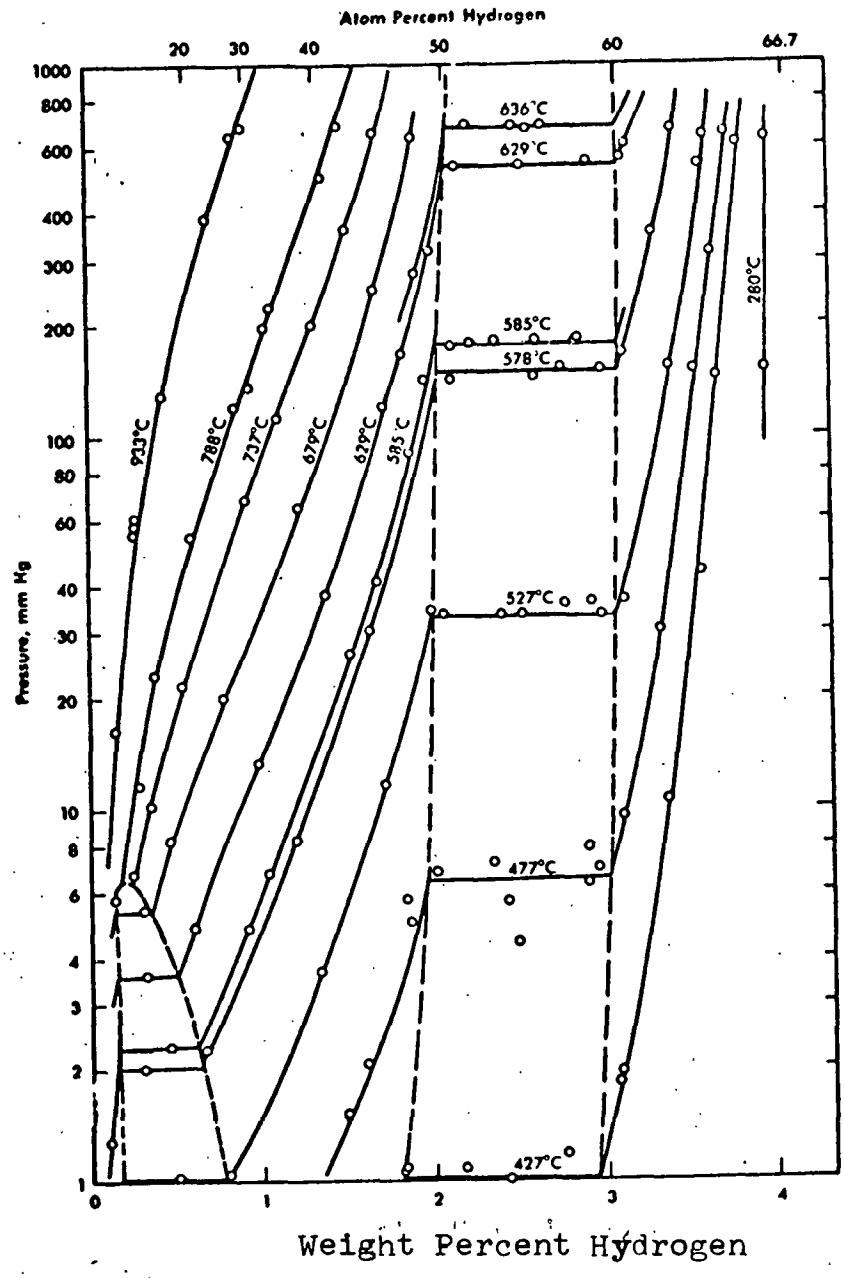

Fig. 11. Equilibrium pressure-temperature-composition data[22] for titanium in the temperature range of interest.

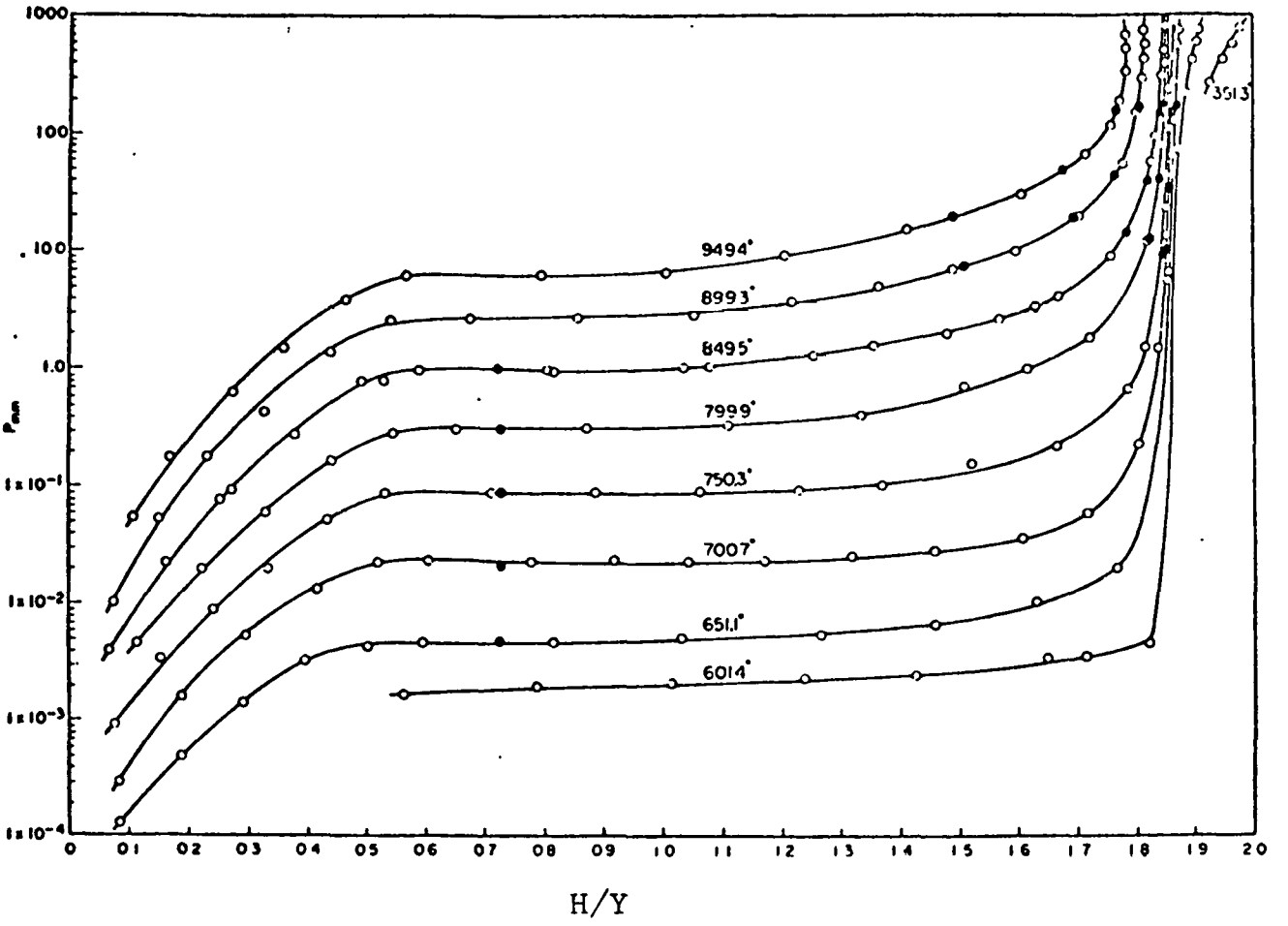

Fig. 12. Equilibrium pressure-temperature-composition data[23] for yttrium in the temperature range of interest.

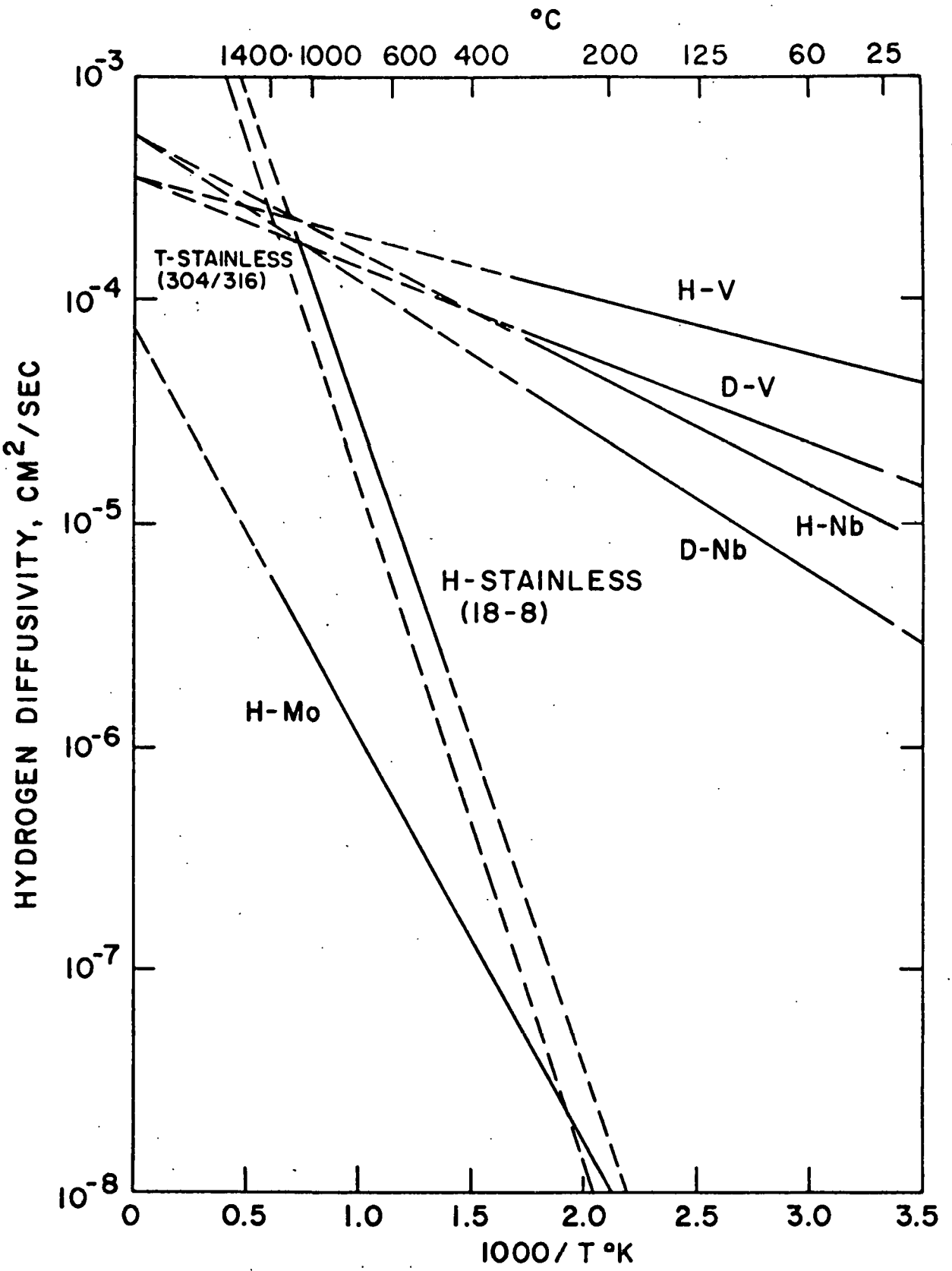

Fig. 13. Diffusivities of hydrogen and its isotopes in the metals indicated. The hydrogen-stainless steel data are from Geller and Sun,[24] the tritium-stainless steel from Austin and Elleman,[25] the molybdenum data from Jones et al.[19] and the niobium and vanadium data are from Völkl et al.[26]

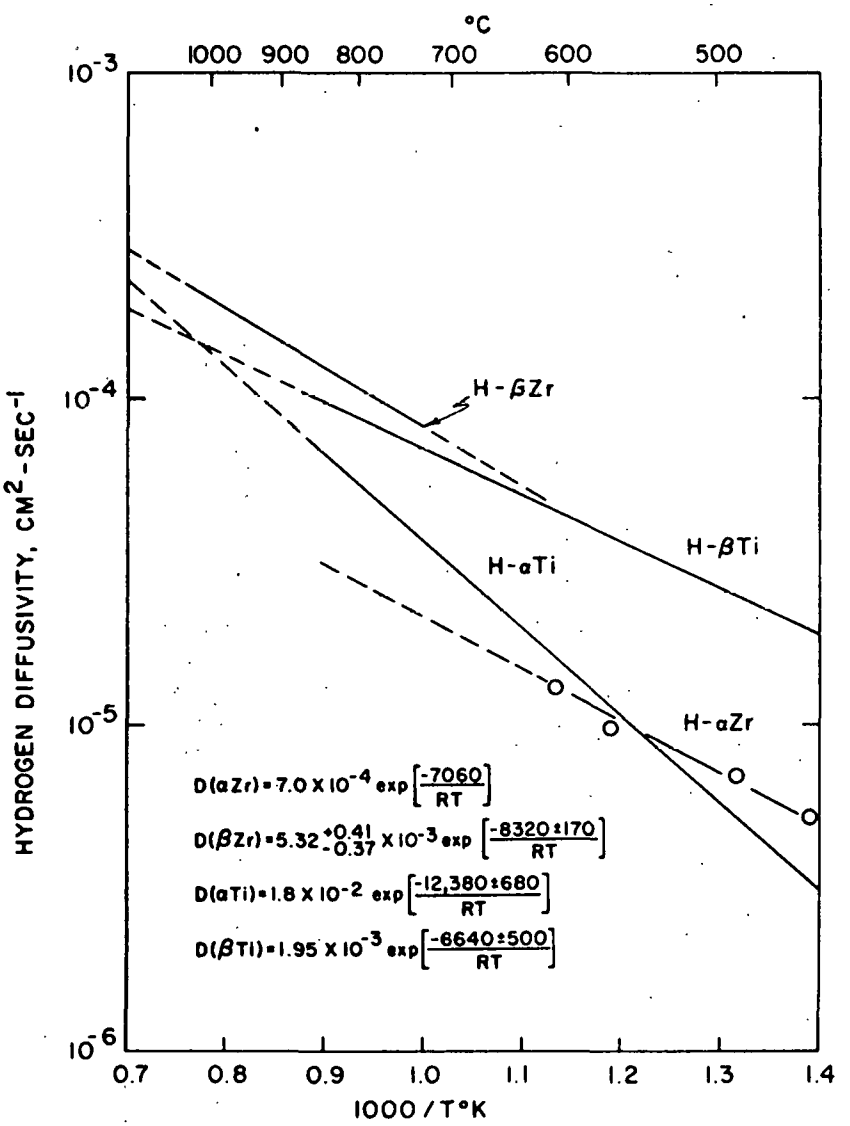

Fig. 14. Diffusivities of hydrogen and its isotopes in the metals indicated. Data for α Zr are from Mallett and Albrecht[27], and for β Zr from Gelezumas et al.[28] while the data for titanium are from Wasilewski and Kehl[29].

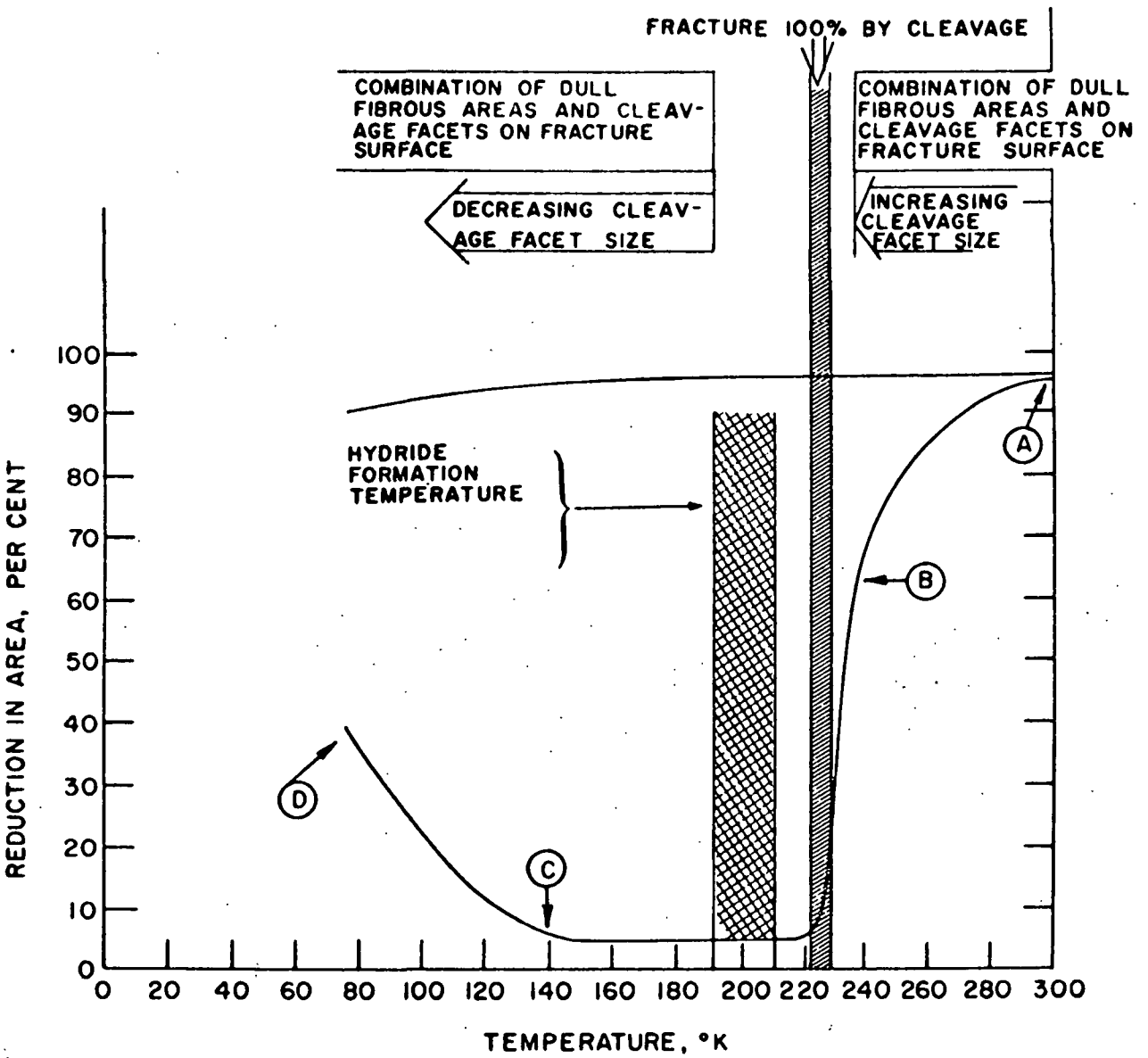

Fig. 15. Schematic illustration of the ductility behavior of hydrogen charged metal depicting four temperature regions, A, B, C and D, of special interest.

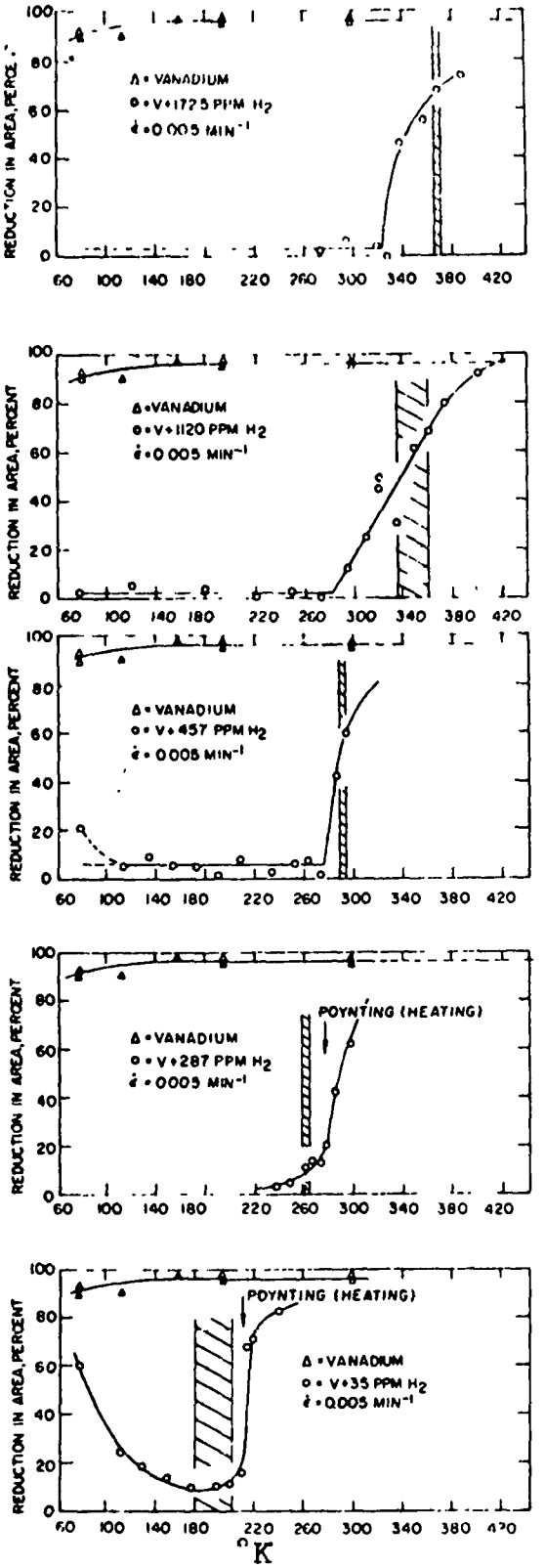

Fig. 16. Ductility of vanadium containing indicated concentrations of hydrogen vs. test temperature showing that the DBTT increases with hydrogen concentration. The cross-hatched region indicates the temperature range of visual observations of hydride formation on cooling.

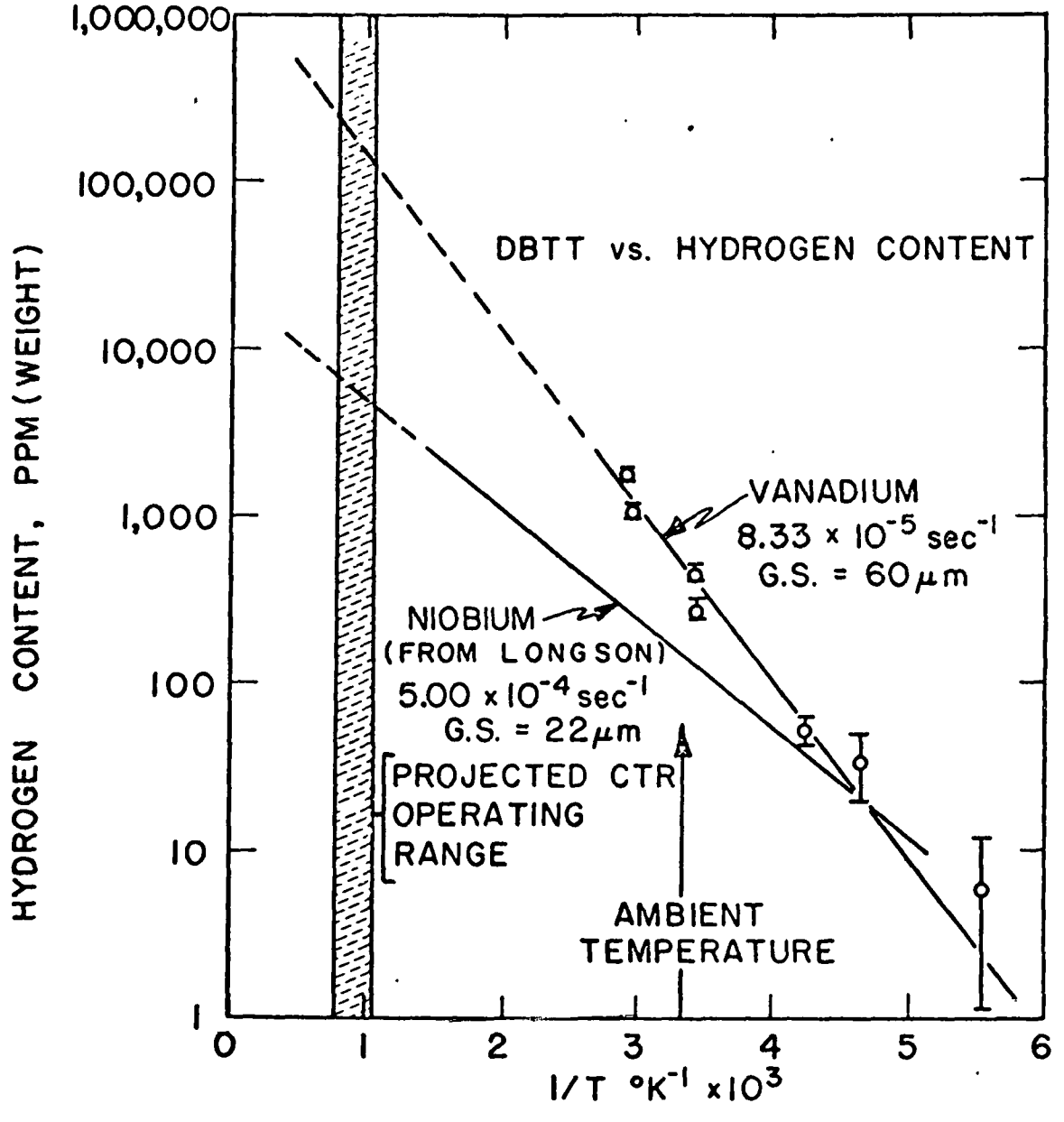

Fig. 17. Relation between hydrogen content and the reciprocal of the DBTT for vanadium. The behavior of niobium is from Longson[42].

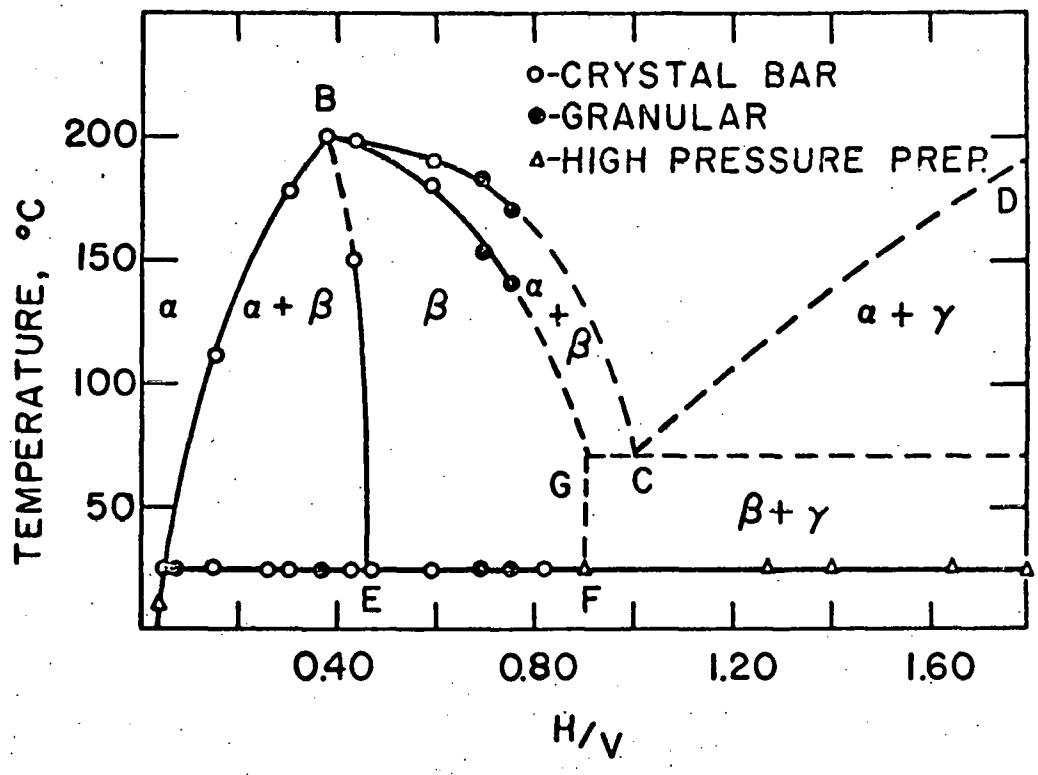

Fig. 18. Phase diagram for the vanadium-hydrogen system given by Maeland[48].

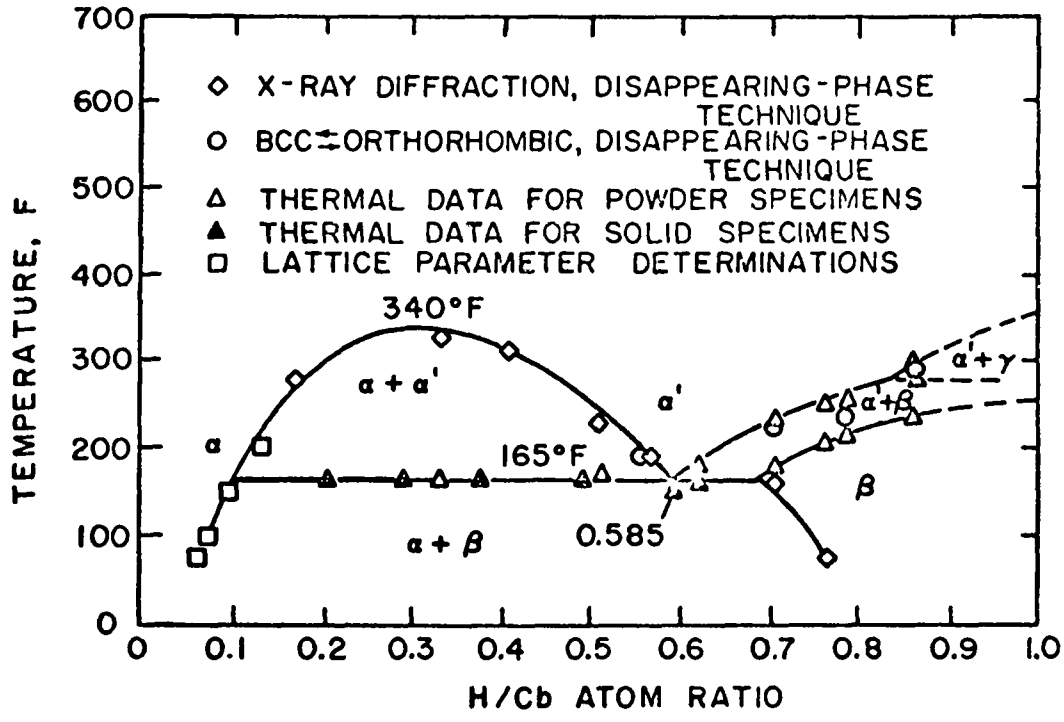

Fig. 19. Phase diagram for the niobium-hydrogen system given by Walter and Chandler[49].

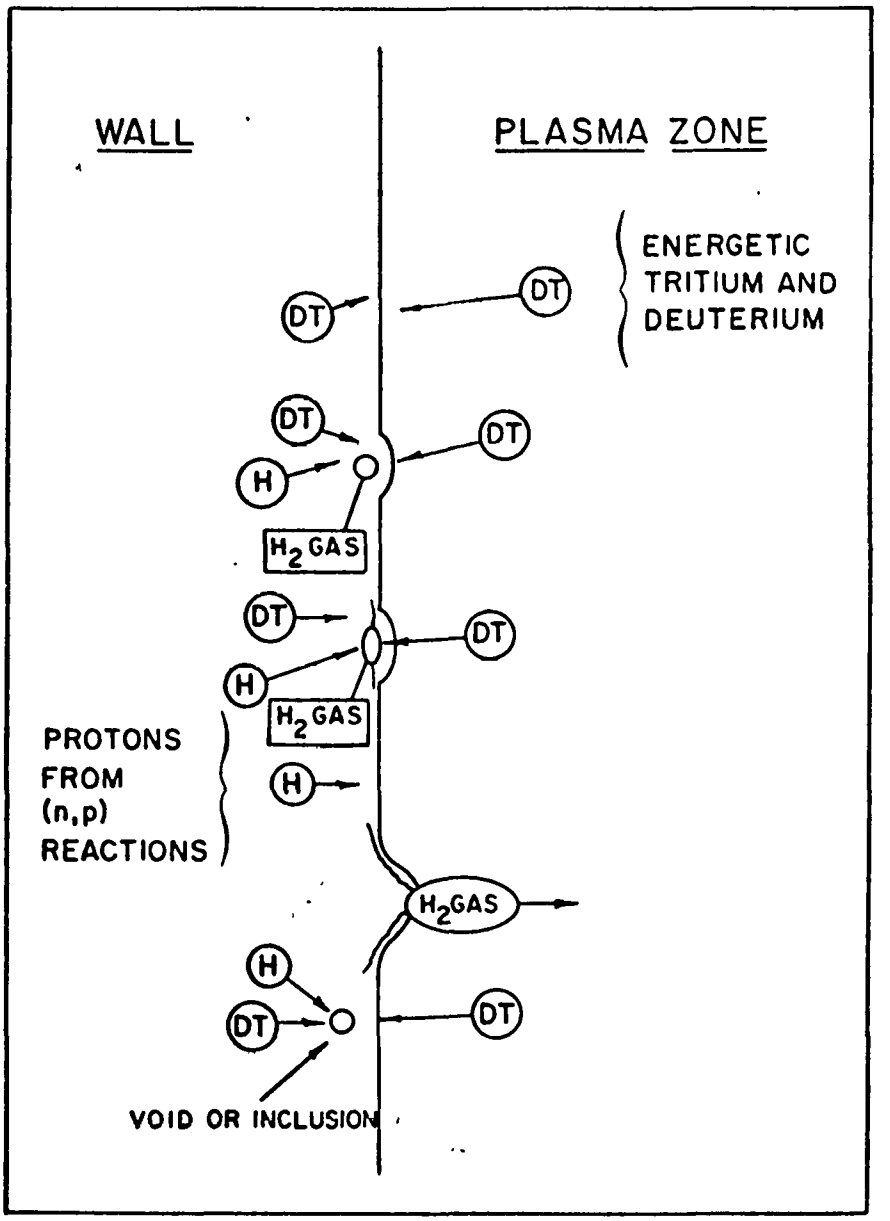

Fig. 20. A schematic illustration of the blistering phenomenon due primarily to injected energetic deuterium and tritium atoms including the contributions from internal hydrogen.

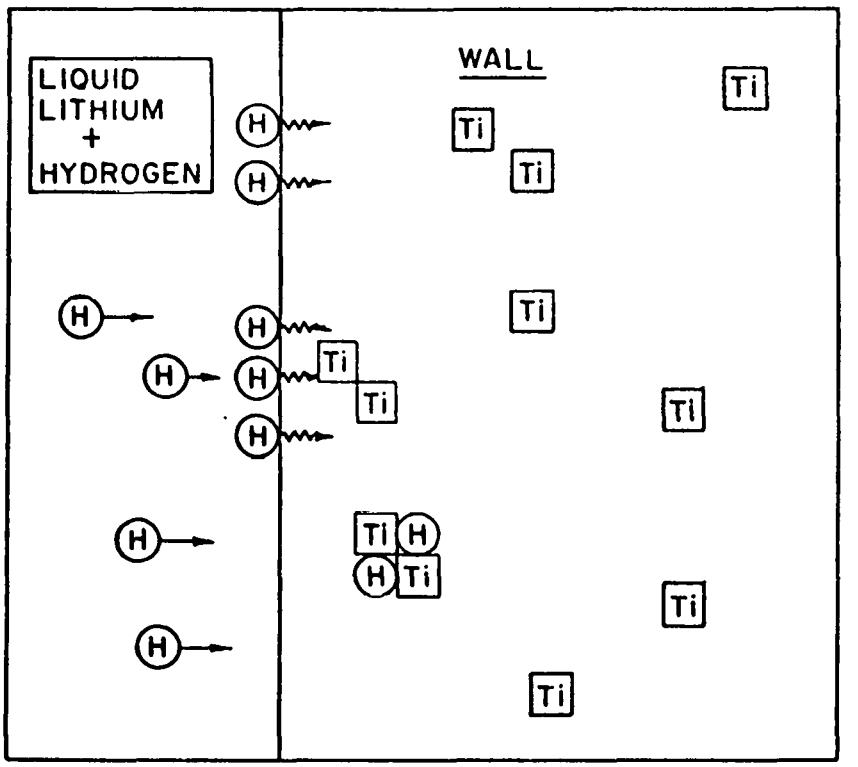

Fig. 21. A schematic illustration of the physical process of internal hydriding using dissolved titanium as the example.

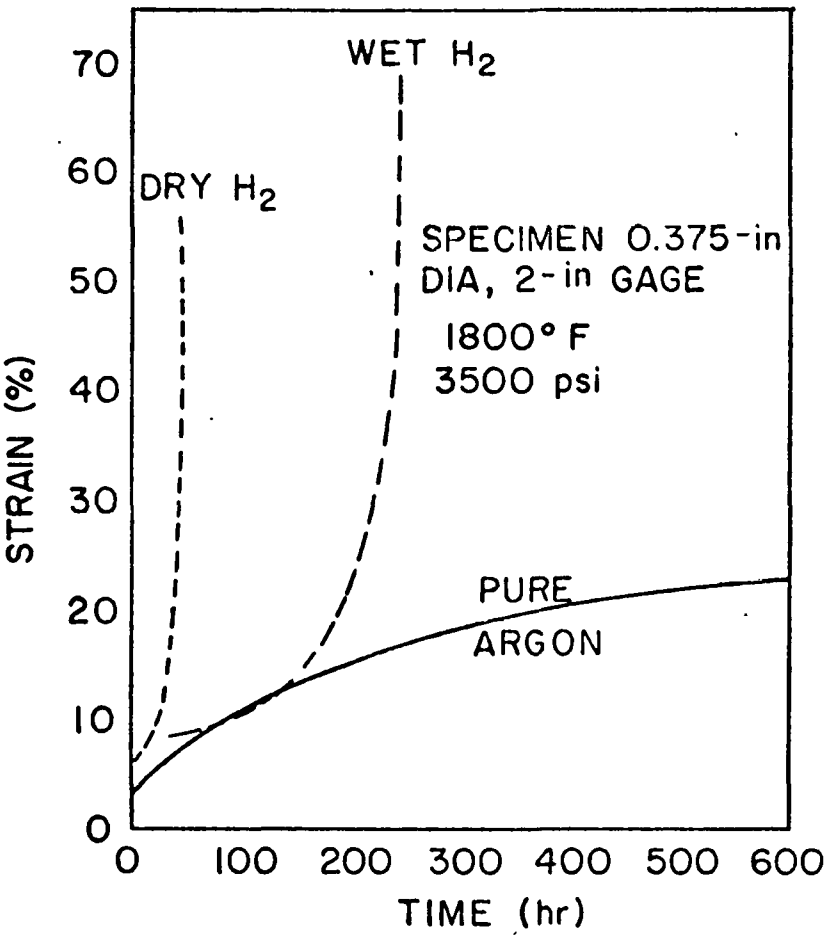

Fig. 22. Experimental results from McCoy and Douglas[115] showing the effect of a hydrogen environment on creep of niobium.

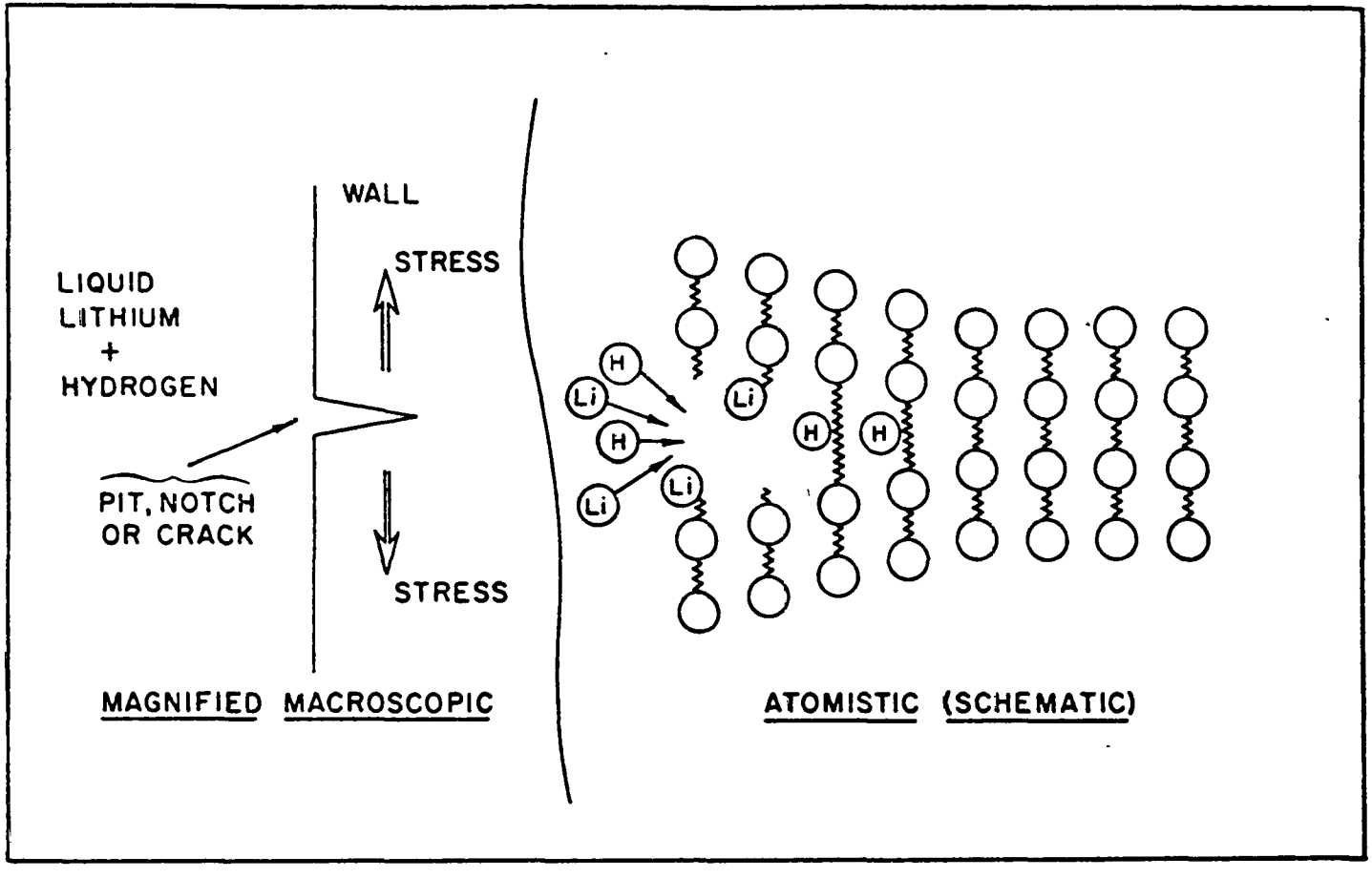

Fig. 23. A schematic illustration of the physical process envisioned for hydrogen atmosphere accelerated crack propagation.